The Canadian Mineralogist
Vol. 31, pp. 821-847 (1993)

RAPAKIVI AND RELATED GRANITOIDS OF THE NAIN PLUTONIC SUITE: GEOCHEMISTRY, MINERAL ASSEMBLAGES AND FLUID EQUILIBRIA

RONALD F. EMSLIE AND JOHN A.R. STIRLING

Geological Survey of Canada, 601 Booth Street, Ottawa, Ontario K1A 0E8

ABSTRACT

Granitoid rocks associated with massif anorthosites in the Nain Plutonic Suite (NPS) of central Labrador display distinctive characteristics in their mineral assemblages, mineral chemistry, and whole-rock chemistry. The principal granitoid plutons of NPS, despite wide areal dispersion, are remarkably similar in major- and trace-element chemistry and display relatively moderate degrees of differentiation. Estimated conditions of late-stage crystallization ranged from about 750° to 800°C, with $f(O_2)$ 1 to 3 log units below FMQ buffer at a total pressure of 3.5 kbar. Low fugacities of water, in the range 250 to 900 bars, estimated from biotite reactions, tend to reflect near-solidus upper limits for the magmas, because petrographic evidence indicates that biotite typically crystallized late. The composition of the magma, rich in Or relative to Ab components, seems to have resulted from reduced activities of water during partial melting of the crustal sources. Chemical and physical properties of magmas and minerals are used to constrain estimates of the conditions [T, P, $f(H_2O)$, viscosity, cooling rate] under which the partial melts initially formed and subsequently evolved, and the nature of source materials and crustal residues. The classic rapakivi texture of plagioclase-mantled perthite is prominent only in the Makhavinekh pluton which, however, is not chemically or otherwise texturally or mineralogically unique. Physical conditions and processes attending emplacement and crystallization were probably decisive factors in development of the texture. Extraction of large volumes of granitic partial melt from the crust left geochemically depleted, hot residues of plagioclase – pyroxene granulite. These residues formed optimal contaminants with which to derive anorthositic magmas through assimilation by contemporary proximal basic magma that supplied the heat.

Keywords: rapakivi, anorthosite, rock chemistry, mineral chemistry, temperature, pressure, oxygen fugacity, water fugacity, partial melting, crustal residues, Nain plutonic suite, Labrador.

SOMMAIRE

Les roches granitiques associées aux anorthosites massives de la suite plutonique de Nain, dans la partie centrale du Labrador, montrent des caractères distinctifs en ce qui concerne les assemblages minéraux, la chimie des minéraux, et celle des roches totales. Malgré leur large dispersion géographique, les principaux plutons granitiques de la suite sont remarquablement semblables par leurs teneurs en éléments majeurs et en traces, et montrent un taux de différenciation relativement faible. L'estimation des conditions de fin de cristallisation conduit à des températures de 750° à 800°C et une fugacité d'oxygène de 1 à 3 unités logarithmiques en-dessous du tampon FMQ pour une pression totale de 350 MPa. Estimées d'après les réactions impliquant la biotite entre 25 et 90 MPa, les faibles fugacités d'eau doivent refléter les conditions maximales proches du solidus des magmas, car les observations pétrographiques indiquent que la biotite a cristallisé tardivement. La composition du liquide magmatique, riche en Or relativement à Ab, paraît résulter d'une activité réduite de l'eau au cours de la fusion partielle de sources crustales. Grâce aux propriétés chimiques et physiques des magmas et des minéraux, il est possible de déduire les valeurs limites pour estimer les conditions dans lesquelles les liquides de fusion partielle se sont formés initialement, puis ont évolué, ainsi que la nature des matériaux sources et des résidus de fusion. La texture rapakivi classique du feldspath mésoperthitique enrobé de plagioclase n'est importante que dans le pluton de Makhavinekh, qui, par ailleurs, ne montre pas de caractères chimiques, pétrographiques ou minéralogiques spécifiques. Les conditions physiques et les processus lors de la mise en place et de la cristallisation sont probablement des facteurs décisifs dans le développement de la texture. L'extraction de grands volumes de liquide granitique par fusion partielle de la croûte conduit à former des résidus appauvris et chauds de granulite à plagioclase – pyroxène. Ces résidus constituent les meilleurs contaminants pour dériver les magmas anorthositiques à partir des magmas basiques contemporains et voisins.

(Traduit par la Rédaction)

Mots-clés: rapakivi, anorthosites, chimie des roches, chimie des minéraux, température, pression, fugacité d'oxygène, fugacité d'eau, fusion partielle, résidu crustal, suite plutonique de Nain, Labrador.

---

* Geological Survey of Canada contribution number 27792. Contribution number 14 to the International Geological Correlation Program, Project 315 on Rapakivi granites and related rocks.

INTRODUCTION

Granitoid intrusions closely associated with the major anorthosite complexes of central and northern Labrador have been recognized for some time as having characteristics similar to classic rapakivi granite associations (Bridgwater & Windley 1973, Emslie 1978, 1991, Anderson 1980, Ryan 1991). The present paper summarizes recently obtained chemical data on rocks and minerals for the larger granitoid intrusions associated with the Nain Plutonic Suite (NPS).

Recent U–Pb (zircon) dating of rocks of the NPS (Simmons *et al.* 1986, Simmons & Simmons 1987, Ryan *et al.* 1991, Emslie & Loveridge 1992) and major complexes of this type elsewhere (*e.g.*, Wiborg batholith, Finland: Vaasjoki *et al.* 1991, Rämö 1991; rapakivi batholiths of southwestern Finland: Suominen 1991; Rogaland, southwestern Norway, Pasteels *et al.* 1979) has demonstrated the close and overlapping ages of crystallization in associated basic, anorthositic, and granitoid compositions. The mineralogy of the granitoids, including the presence of pyroxenes and fayalite in earlier-crystallized members of many suites, points to relatively high temperatures of early crystallization and water-poor magmas. This is in accord with a close association with basic magmas that acted as major sources of heat.

Three large granitoid bodies associated with the NPS, the Umiakovik Lake batholith, the Makhavinekh pluton, and the Notakwanon batholith are the principal focus of this study; also included are some comparative data from the Mistastin batholith, which is some 100 m.y. older but similar petrographically, chemically, and in rock associations. Emphasis in the present study is placed on mineral assemblages and compositions that bear most directly on derivation of useful estimates of intensive variables T, P and fluid compositions that prevailed during formation and crystallization of the granitoid magmas.

The presence of fayalitic olivine with high-Ca and, rarely, low-Ca pyroxenes, is common in many of the granitoid associations with anorthositic rocks in Labrador and elsewhere. Hornblende and biotite stabilities increase relative to anhydrous mafic silicates as water activities increase and temperature declines in evolving granitic melts (Naney 1983, Clemens *et al.* 1986, Puziewicz & Johannes 1990). Many associations have biotite – hornblende in addition to olivine- and pyroxene-bearing facies, and petrographic evidence of anhydrous ferromagnesian minerals rimmed by biotite and hornblende is common. The clear implication is that, as a general rule, water activities rose as crystallization of anhydrous minerals proceeded. Orthopyroxene occurs sporadically in these granitoids, so they are only in part strictly charnockitic. However, the lower-pressure equivalent assemblage, fayalitic olivine + quartz, is widespread, implying that pressures of crystallization slightly below that required to stabilize ferrosilite relative to fayalite + quartz was the only important factor preventing wider development of charnockites in the strict sense.

Recent investigations (Nekvasil 1990, 1991, Stimac & Wark 1992) have clarified some of the controls leading to the development of a plagioclase mantle on K-feldspar to form the classic rapakivi texture. In the Nain Plutonic Suite, only the Makhavinekh pluton displays widespread mantling of perthite ovoids by plagioclase, and geochemical and petrological reasons are sought to explain this phenomenon.

The existence of penecontemporaneous basic and granitic magmatism in NPS demands that greater efforts be made to test petrogenetic models that relate various members of the suite more rigorously. Because the granitoid rocks comprise about half of the outcrop area of NPS, the details of their genesis must be intimately linked to that of other members of the suite; aspects of that relationship are explored in this paper.

GEOLOGY

The Nain Plutonic Suite is a prominent example of widespread mid-Proterozoic Elsonian magmatism in central Labrador. Early studies by Wheeler (1933, 1942, 1955, 1960) and later efforts in collaboration with coworkers (S.A. Morse, D. deWaard, J.H. Berg and many others), plus more recent investigations by R.A. Wiebe and coworkers, have formed a solid basis for the pursuit of a more detailed understanding of the genesis and development of this remarkable igneous complex.

The NPS intrudes the boundary region between the Nain Province and the Churchill (Rae) Province to the west (Fig. 1). Nd and Sr isotopic signatures in basic igneous rocks of the NPS distinguish contamination by older Archean rocks of the Nain Province from that by late Archean and early Proterozoic rocks of the Churchill Province (*e.g.*, Ashwal *et al.* 1988, Emslie & Thériault 1991, Hamilton & Shirey 1992). Although the extent to which the isotopic signatures in basic and anorthositic rocks may reflect effects of the lithospheric source, as opposed to subsequent processes of crustal contamination, remains to be clarified, their potential usefulness in constraining the operative igneous processes is unquestioned.

Currently available U–Pb ages place the minimum time-span of intrusion of the NPS from at least 1.29 to 1.32 Ga [see Emslie & Loveridge (1992) for a recent review]. Although cross-cutting relations of anorthositic by granitoid rocks ("adamellite" in the terminology of Wheeler) were recognized by Wheeler (1955) and subsequent investigators, showing that granitoid rocks were at least in part younger, more recent results of high-precision dating indicate that

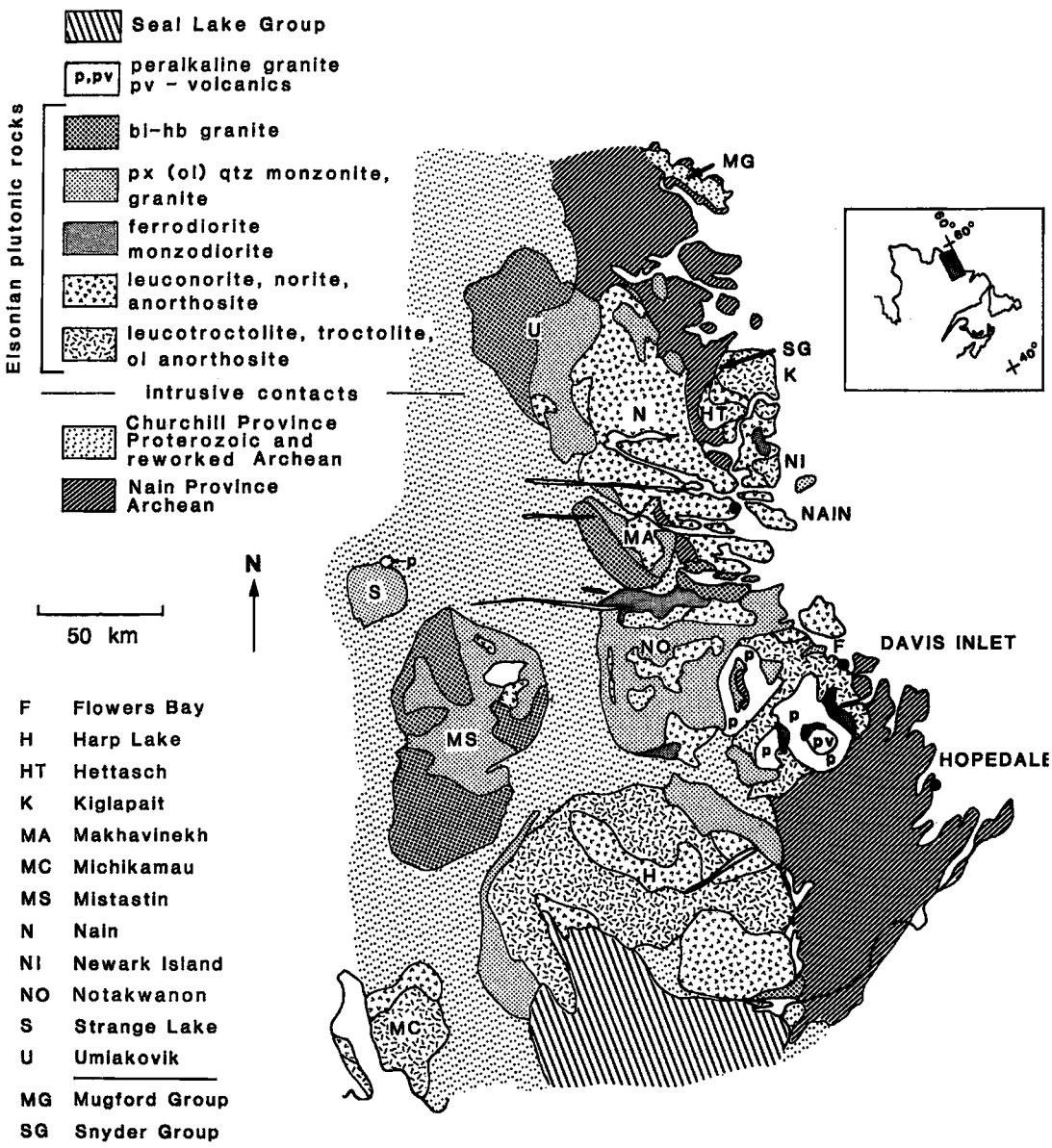

FIG. 1. Geological sketch map of central Labrador showing distribution of principal Elsonian intrusions. The Mugford and Snyder Groups are early Proterozoic supracrustal sequences.

granitic, basic, and anorthositic rocks overlap in ages of crystallization. At present, the oldest published U–Pb zircon ages are from granitoid rocks on the western flanks of the NPS (Ryan *et al.* 1991, Emslie & Loveridge 1991, 1992).

U–Pb zircon dating of two distinct intrusive phases of the Umiakovik Lake batholith yielded similar ages, within experimental error, of about 1.32 Ga, inferred to be the age of igneous crystallization (Emslie & Loveridge 1992). This age is in good agreement with the work of others in the central and southern Nain complex using U–Pb systematics in zircon and other isotopic systems, many recent determinations lying between about 1.30 and 1.32 Ga (*e.g.*, Simmons *et al.* 1986, Simmons & Simmons 1987, Ryan *et al.* 1991).

The Umiakovik Lake batholith

Examination of most parts of the batholith in 1987 and 1989 yielded broad agreement with Wheeler's (1969) indicated distribution of fayalite-, hornblende-, and biotite-bearing facies. A zonal relationship exists such that fayalite- and pyroxene-bearing facies preferentially form a relatively broad zone adjacent to the massif anorthosites to the east (Fig. 2); only rare occurrences are present along the western margin. Monzodiorite is present sporadically only adjacent to anorthosite where, with increasing amounts of perthite megacrysts, it grades into (fayalite)–pyroxene quartz monzonite. Farther from the anorthosite contact, fayalite and pyroxene become rare or absent, and hornblende (typically poikilitic) is the dominant mafic silicate, with only minor biotite present. Biotite-rich facies lie distant from the main anorthosite contact, the largest body of hornblende–biotite granite being in the vicinity of Umiakovik Lake (Wheeler 1969, Emslie & Russell 1988).

Boundaries between fayalite-, pyroxene-, and hornblende-bearing varieties are commonly gradational over substantial distances (tens to hundreds of meters). Hornblende – biotite and biotite granites, on the other hand, are clearly younger and locally intrude fayalite- and pyroxene-bearing varieties as dykes and sheets. Although ovoid perthite grains up to 2 cm or more across are present in places, the mantled rapakivi texture is absent in the Umiakovik Lake batholith.

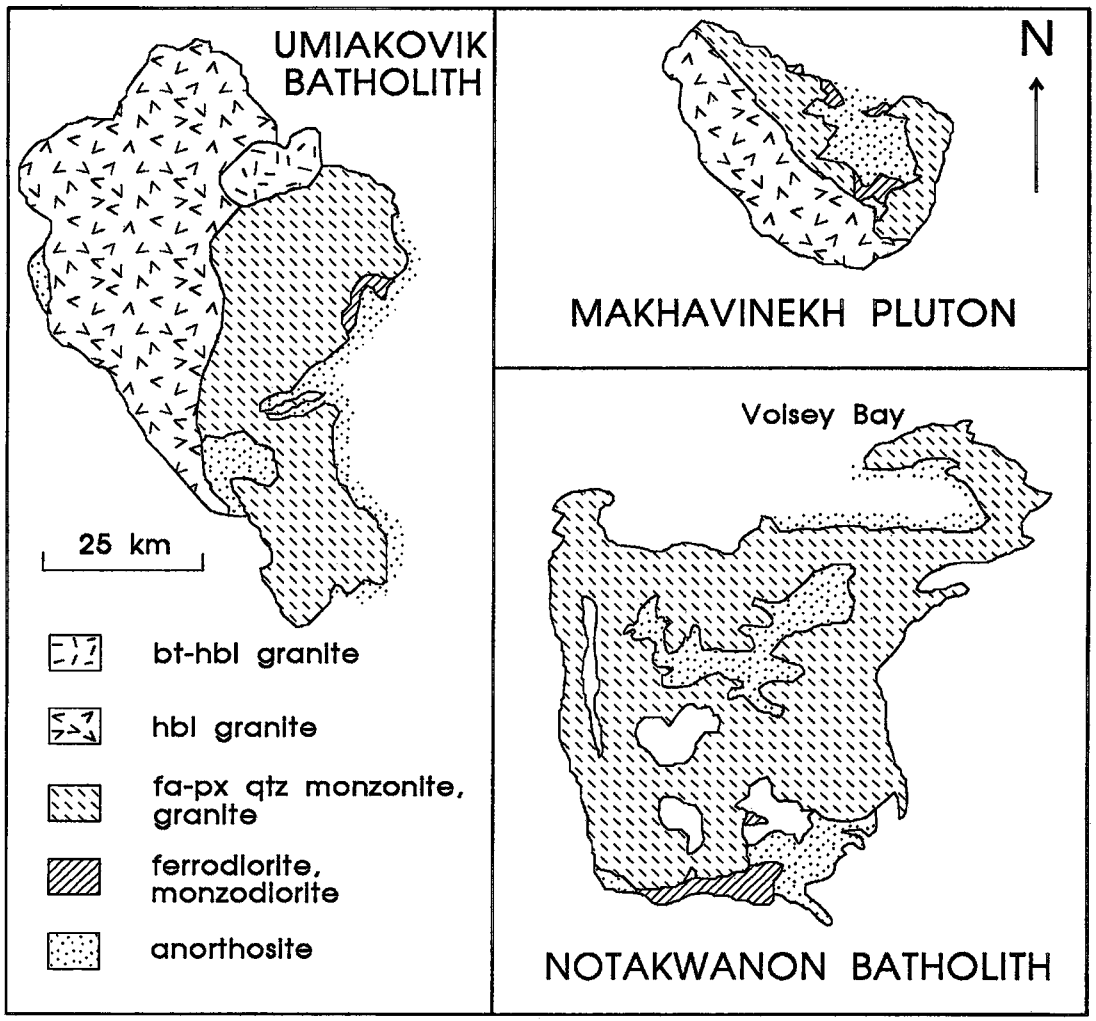

FIG. 2. More detailed maps of the principal granitoid intrusions of the Nain Plutonic Suite, the Umiakovik batholith, Makhavinekh pluton and Notakwanon batholith.

A whole-rock Rb–Sr isochron age of 1290 ± 37 Ma, Sr_i= 0.7096 ± 0.0013 (using an ^{87}Rb decay constant of 1.42 × 10^{-11} yr^{-1}) has been reported (Taylor 1978) for granitic rocks of the Umiakovik Lake batholith. This is some 30 Ma younger than recent U–Pb (zircon) ages measured for the batholith (Emslie & Loveridge 1992), a result in accord with protracted cooling in a crustal regime of high heat flow, as also suggested by hornblende and biotite ages from the batholith (Emslie 1987).

The Makhavinekh pluton

This igneous complex, recently described by Ryan (1991), contains two gradational granitoid units that appear to overlie anorthosite and associated ferrodioritic rocks that are exposed in the interior of the pluton (Fig. 2). Adjacent to the anorthositic rocks, a fayalite – augite – hornblende-bearing facies of quartz monzonite grades distally into (biotite)–hornblende granite. Some local evidence of mixing is present between underlying ferrodiorite and overlying quartz monzonite (Ryan 1991). Of the large granitoid plutons within the Nain Plutonic Suite, only the Makhavinekh pluton shows an abundant development of the rapakivi texture (Ryan 1991).

The Notakwanon batholith (Notakwanon – Voisey Bay)

This igneous association has been described by Hill (1982). It is similar in many respects to the others, but tends generally to be less coarse-grained, in part porphyritic, more quartz-rich and has wider distribution of fayalitic olivine. Units characterized as granite, quartz monzonite, quartz syenite, and porphyritic granite have been described by Hill. It is older, but perhaps only slightly, than the peralkaline granites of the Flowers River complex that intrude it (Hill 1982).

The Mistastin batholith

This is the largest of the Elsonian granitoid complexes in central Labrador (Fig. 1). It is dominated by older pyroxene quartz monzonite intruded by younger biotite – hornblende granite; a small body of fayalite quartz syenite intrudes the granite. Crystallization of the batholith took place about 1.42 Ga ago based on U–Pb (zircon) dating (J.C. Roddick, pers. comm., 1990), and thus significantly predates the crystallization of at least some, and probably all, of the Nain complex. Mineral data from the Mistastin batholith are considered here for comparative purposes only.

Mineralogy and Geochemistry

Analytical techniques

Rock powders were prepared from splits of samples weighing 2 to 4 kg. Whole-rock chemical analyses were performed by staff of the Analytical Chemistry laboratories of the Geological Survey of Canada. Concentrations of the major elements and the trace elements Sr, Rb, Nb, Ba, Zr were determined by wavelength-dispersion X-ray fluorescence (XRF) techniques supplemented by rapid wet-chemical methods. Trace-element analysis was performed by a combination of wavelength-dispersion XRF methods and by inductively coupled plasma combined with emission spectroscopy (ICP–ES) on solutions prepared from 1 g of sample. Concentrations of the *REE* were determined by ICP–ES and inductively coupled plasma combined with mass spectrometry (ICP–MS) on solutions concentrated using an ion-exchange resin.

Mineral analyses were carried out on a Cameca SX–50 electron microprobe using wavelength-dispersion techniques, with counting times of 10 to 20 seconds. The analytical conditions, 15 kV, with sample currents 10 to 30 nA, were considered appropriate for the minerals analyzed. We used a variety of natural and synthetic standards. Raw data were corrected with the model of Pouchou & Pichoir (1984). Lower beam-currents and longer counting-times were used to avoid volatilization of elements of low atomic number. In the case of feldspars, a defocused spot of up to 15 μm was used where grain size permitted. Oxygen concentrations were quantitatively monitored as a check on analytical totals. The effects of the carbon coating on intensity of the O peak was overcome by coating the standard for O (quartz) along with the sample. Compositions of minerals obtained by electron-microprobe analysis (Appendix 1) are available from the Depository of Unpublished Data, CISTI, National Research Council, Ottawa, Ontario K1A 0S2. The location of all samples analyzed is recorded in Appendix 2.

Petrography

Mineral associations observed petrographically in all of the granitoid plutonic bodies are remarkably similar. Perthitic K-feldspar, plagioclase, and quartz are essential minerals in all rocks except monzonites and monzodiorites that lack quartz. Fayalite and augite, locally accompanied by pigeonite or orthopyroxene or both, are typical ferromagnesian silicates of the earlier members. Hornblende becomes gradually more abundant, first as a rim and as flecks permeating augite along cleavages, then as larger discrete grains and plates that may exhibit relict kernels of pyroxene or olivine at their core. Biotite typically displays

TABLE 1. MAJOR- AND TRACE-ELEMENT CHEMISTRY OF THE GRANITOID ROCKS

	Umiakovik batholith								Nakhavinekh pluton				Voisey Bay - Zoar				Notakwanon									
Rock Type	monzod n=10		faypxqm n=14		hbqm n=14		bihbgr n=11		olhbgr n=7		hbgran n=8		Gp a n=5		Gp b n=5		unit 16b n=7		unit 16c n=10		unit 16a n=13		1989 GpA n=3		1989 GpB n=7	
	mean	s	mean	s	mean	s	mean	s	mean	s	mean	s	mean	s	mean	s	mean	s	mean	s	mean	s	mean	s	mean	s
wt%																										
SiO2	50.45	3.90	65.86	2.21	67.71	0.91	72.20	1.72	68.26	2.68	70.74	1.28	67.60	3.62	74.46	1.44	50.28	3.05	66.70	4.17	69.92	2.60	71.17	1.82	74.26	0.74
TiO2	2.88	0.99	0.99	0.25	0.84	0.11	0.52	0.19	0.66	0.16	0.48	0.08	0.96	0.43	0.40	0.09	1.48	0.55	0.95	0.38	0.62	0.27	0.50	0.11	0.29	0.04
Al2O3	13.99	1.74	13.31	0.67	13.12	0.37	12.68	0.30	13.50	0.86	12.99	0.53	13.00	0.71	12.30	0.75	13.44	0.76	12.69	0.41	12.74	0.42	12.90	0.53	12.01	0.23
Fe2O3	1.61	0.62	1.74	0.32	1.49	0.22	0.86	0.42	1.68	0.51	1.20	0.21	1.10	0.23	0.42	0.25	-	-	-	-	-	-	1.27	0.42	1.60	0.22
FeO	14.89	4.07	5.95	1.76	4.86	0.52	2.96	1.00	4.07	1.41	3.10	0.52	5.70	2.32	2.46	0.62	10.23	2.50	7.03	2.70	4.96	1.81	3.27	0.66	1.46	0.22
MnO	0.22	0.06	0.09	0.03	0.07	0.02	0.04	0.02	0.07	0.02	0.05	0.01	0.09	0.03	0.04	0.01	0.14	0.03	0.10	0.03	0.06	0.02	0.05	0.01	0.03	0.01
MgO	2.62	1.06	0.65	0.22	0.63	0.16	0.38	0.14	0.29	0.11	0.32	0.05	0.76	0.28	0.36	0.10	0.95	0.70	0.55	0.28	0.22	0.21	0.21	0.10	0.10	0.02
CaO	7.45	0.86	3.31	0.66	2.57	0.44	1.54	0.61	1.65	0.72	1.63	0.34	2.81	0.48	1.22	0.22	4.30	1.11	2.82	1.10	1.96	0.81	1.50	0.51	0.70	0.17
Na2O	2.88	0.26	2.94	0.21	2.98	0.17	2.80	0.22	3.00	0.36	2.91	0.12	3.50	0.28	3.32	0.20	3.77	0.54	3.29	0.24	3.51	0.16	3.53	0.42	3.44	0.30
K2O	1.24	0.56	4.06	0.62	4.48	0.22	5.07	0.63	4.62	0.43	5.38	0.48	3.63	0.10	4.38	0.22	3.79	1.02	4.23	0.54	4.82	0.63	4.90	0.63	5.23	0.20
P2O5	0.84	0.46	0.29	0.08	0.23	0.04	0.11	0.06	0.17	0.06	0.10	0.03	0.23	0.10	0.07	0.03	0.34	0.27	0.25	0.13	0.11	0.08	0.08	0.05	0.02	0.01
H2O	0.43	0.08	0.56	0.11	0.82	0.22	0.58	0.19	0.40	0.10	0.65	0.10	0.42	0.08	0.34	0.11	-	-	-	-	-	-	0.43	0.06	0.50	0.21
CO2	0.22	0.20	0.17	0.11	0.15	0.08	0.13	0.09	0.10	-	0.12	0.04	0.06	0.09	0.08	0.04	-	-	-	-	-	-	0.17	0.06	0.17	0.05
S	0.13	0.09	0.03	0.02	0.01	0.01	0.01	0.01	0.01	0.01	0.01	0.01	0.03	0.02	0.00	0.01	-	-	-	-	-	-	0.20	0.02	0.00	0.00
Total	99.85		99.95		99.96		99.88		98.48		99.68		99.89		99.85		98.72		98.61		98.92		100.18		99.81	
ppm F	839	334	956	317	1220	258	819	244	434	147	1054	339	797	271	983	495	682	273	828	359	521	300	540	158	1571	683
Cl	279	83	291	122	367	55	374	104	-	-	181	61	356	68	449	112	-	-	-	-	-	-	194	-	225	108
Cr	26	21	8	3	5	2	8	5	3	1	3	1	3	1	4	3	-	-	-	-	-	-	5	1	3	2
Ni	11	8	1	1	-	-	2	2	-	-	-	-	-	-	-	-	-	-	-	-	-	-	-	-	-	-
Co	33	6	14	5	12	3	7	3	5	2	4	1	8	3	3	1	-	-	-	-	-	-	4.7	2.9	1	0.8
V	133	83	21	11	18	12	15	13	28	13	5	3	15	10	3	3	-	-	-	-	-	-	-	-	-	-
Cu	20	10	8	2	6	3	5	3	8	4	5	2	13	5	6	1	-	-	-	-	-	-	6	3	5	1
Zn	183	70	126	28	101	14	69	29	108	25	88	21	99	40	46	15	176	46	-	-	-	-	90	22	90	20
Rb	19	13	87	17	116	22	133	32	74	10	107	20	61	10	99	43	73	28	131	53	144	57	103	13	178	11
Ba	838	386	1782	242	1485	186	1234	402	2506	631	2207	509	2060	182	1130	460	1922	1238	1298	193	1361	202	1433	58	593	390
Sr	403	77	241	49	216	28	158	34	231	65	189	49	272	35	140	28	214	57	159	21	124	43	102	45	31	21
Nb	20.0	11.0	20.0	6.0	20.0	5.6	16.0	6.8	14.3	1.8	21.0	5.4	6.3	2.9	8.3	5.8	49.0	-	-	-	-	-	25.0	6.2	40.0	12.6
Be	1.3	0.3	2.3	0.4	2.8	0.5	2.3	0.6	1.8	0.6	2.4	0.6	1.9	0.4	2.3	0.8	-	-	-	-	-	-	2.0	0.4	4.0	0.8
Zr	470	350	677	135	565	34	496	126	653	84	586	90	720	269	488	156	816	342	569	97	599	195	740	313	616	115
Y	41.0	10.6	56.0	13.8	54.0	11.3	47.0	11.9	39.6	8.2	54.0	12.2	44.6	14.4	33.4	5.3	92.0	-	-	-	-	-	39.3	8.5	66.0	12.0
La	41.5	17.5	74.6	12.2	86.1	10.8	70.4	23.7	51.0	11.4	83.0	22.0	68.6	15.3	77.8	12.1	-	-	-	-	-	-	62.7	14.6	123.0	31.0
Ce	89.4	40.4	156.0	25.6	174.0	22.1	144.0	45.4	96.0	27.8	166.0	45.0	134.0	33.6	151.0	18.9	252.0	-	-	-	-	-	128.0	33.0	238.0	54.0
Nd	56.2	29.3	78.0	11.8	82.5	9.0	66.1	18.6	52.3	21.6	73.0	22.0	58.6	21.5	49.8	6.1	-	-	-	-	-	-	62.7	13.6	97.0	19.4
Sm	12.5	6.2	15.1	2.3	15.3	1.9	11.5	2.8	10.1	3.4	12.9	3.8	12.8	4.1	9.9	1.6	-	-	-	-	-	-	11.2	2.4	16.3	3.4
Eu	3.3	1.2	3.0	0.3	2.6	0.2	2.0	0.5	3.6	0.8	3.0	0.6	3.0	0.2	1.6	0.6	-	-	-	-	-	-	1.9	0.2	1.1	0.2
Gd	11.1	5.4	12.7	2.1	12.7	1.5	9.8	2.6	9.1	2.7	11.0	2.7	10.8	3.5	7.8	1.6	-	-	-	-	-	-	9.5	1.8	13.6	3.1
Dy	8.7	3.1	11.0	2.4	11.0	1.7	8.8	2.3	7.6	2.2	10.0	2.5	9.3	3.2	6.3	1.3	-	-	-	-	-	-	8.4	1.6	12.8	2.9
Yb	3.6	1.0	5.4	1.5	5.3	1.4	4.5	1.2	3.9	1.1	5.4	1.4	4.9	1.5	3.8	0.8	-	-	-	-	-	-	4.2	1.4	7.2	1.4
Norms wt%																										
q	3.8		23.2		25.2		31.4		25.9		28.2		24.0		34.0		9.0		21.3		24.3		27.3		32.8	
c	0.0		0.0		0.0		0.1		0.0		0.0		0.0		0.0		0.0		0.0		0.0		0.0		0.0	
or	7.4		24.2		26.8		30.2		27.6		32.2		21.6		26.1		22.7		25.4		28.8		29.2		31.2	
ab	24.6		25.1		25.5		23.9		25.7		24.9		29.8		28.3		32.3		28.2		30.0		30.1		29.4	
an	21.8		11.2		9.3		7.0		9.8		6.6		9.1		5.6		8.7		7.5		4.8		4.9		1.9	
di	2.2		0.6		0.4		0.0		0.3		0.2		0.6		0.0		1.3		0.5		0.3		0.2		0.3	
he	6.4		2.4		1.4		0.0		1.8		0.7		2.3		0.0		8.0		3.9		3.5		1.6		1.0	
en	5.6		1.4		1.4		1.0		0.6		0.7		1.6		0.9		1.8		1.1		0.4		0.4		0.1	
fs	18.5		6.8		5.8		4.0		4.2		3.7		7.0		3.6		12.5		9.6		6.4		3.4		0.4	
mt	2.4		2.5		2.2		1.3		2.5		1.8		1.6		0.6		0.0		0.0		0.0		1.9		2.3	
il	5.5		1.9		1.6		1.0		1.3		0.9		1.8		0.8		2.9		1.8		1.2		1.0		0.6	
ap	2.0		0.7		0.5		0.3		0.4		0.2		0.5		0.2		0.8		0.6		0.3		0.2		0.1	

Notes: Units from the Makhavinekh pluton include data from Ryan (1991). Units 16a, 16b, and 16c of the Notakwanon batholith are from Hill (1982). Groupings of higher- and lower-silica subunits in the Voisey Bay – Zoar area (Gpa, Gpb) and for the Notakwanon batholith (1989 GpA, 1989 GpB) are arbitrary.

evidence of late-stage growth, as poikilitic grains and commonly as a fringe around ilmenite that could be near-solidus or subsolidus in origin. Subequant to rounded to drop-like quartz grains are common, together with interstitial grains; quartz is rarely only an interstitial mineral.

Accessory minerals also are similar in all groups. Apatite and zircon are common, allanite less so, titanite is very rare, and topaz is abundant in one late dyke in the Umiakovik batholith. Ilmenite is almost invariably the sole Fe–Ti oxide mineral. Fluorite is widespread, but sporadic in occurrence.

Our petrographic examinations have revealed a number of seemingly completely fresh samples from the Umiakovik Lake and the Mistastin batholiths that contain rare interstitial carbonate grains. These may be products of primary igneous crystallization and, if so, suggest a CO_2 component among fluids dissolved in the magmas.

The classic rapakivi or wiborgite texture of oligoclase-mantled perthite ovoids is widely developed only in the Makhavinekh pluton (Ryan 1991) and in the Mistastin batholith to the west (Emslie *et al.* 1980, Taylor 1979). The great similarity in mineral assemblages in all of the large granitoid masses offers little guidance toward explaining the presence or absence of plagioclase mantling. Unmantled perthite ovoids ("pyterlites" in the Finnish literature) occur widely but sporadically in many of the granitoid bodies.

The mantling of anhydrous ferromagnesian silicates by hydrous ones and the presence of more than one generation of quartz and feldspars strongly suggest lack of equilibrium at the hand-specimen level. This creates difficulties in assessing which mineral equilibria are appropriately applied to a given temperature and pressure, a subject considered further below.

Rock chemistry

The major- and trace-element chemistry of the principal felsic units of NPS is summarized in Table 1. The major-element chemistry of all the granitoid suites is remarkably similar and characterized by enrichment in ferrous iron and in potassium, and depletion in magnesium. With respect to strongly fractionated late-orogenic, postorogenic and anorogenic A-type granites, the trace elements Zr, Ba, Sr, and F are relatively enriched, whereas Rb, the transition elements, and Cl are relatively depleted (*e.g.*, Emslie 1991).

The ratio of concentration of an incompatible to that of a compatible element, such as K and Ti, respectively, can be used as a measure of degree of fractionation. The ratio K/Ti is high (>5) in these granites as for most granitoid rocks. On the other hand, the ratio K/Ti is consistently very low (<2) in NPS ferrodiorites and monzodiorites. In Figure 3, K/Ti is plotted against the proportion of SiO_2, TiO_2, and CaO for the grani-

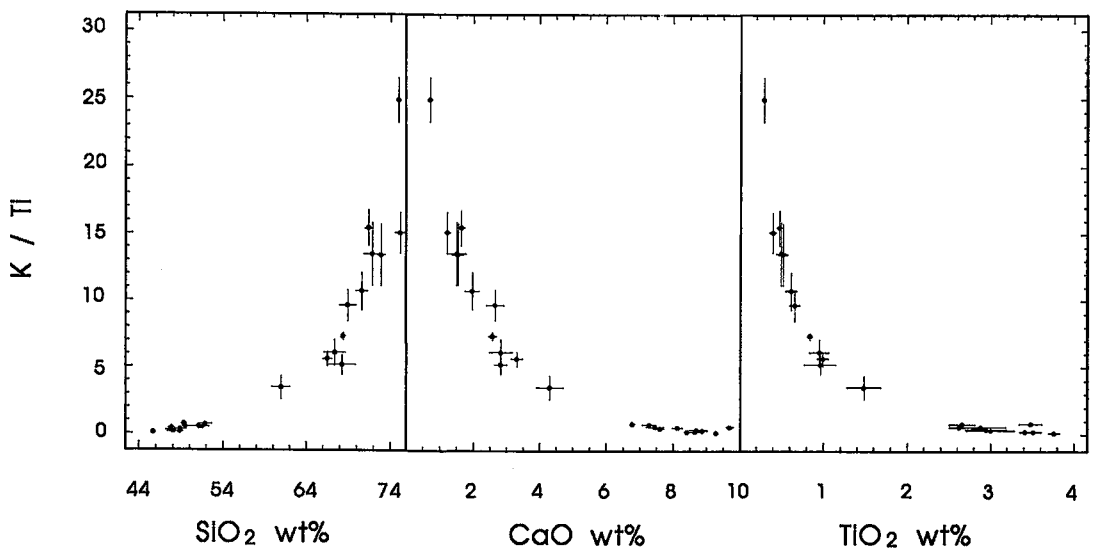

FIG. 3. K/Ti (wt%) plotted against the oxides SiO_2, CaO and TiO_2 for two rock groups of the NPS, the granitoids considered in this paper and diorites (ferrodiorites and monzodiorites). In all plots, the dioritic rocks are tightly clustered at very low K/Ti, whereas the granitoids show regular distribution over a large compositional range. Data for granitoids from Table 1, for diorites from Wiebe & Wild (1983), Wiebe (1978) and Emslie (unpubl. data). Bars indicate one standard error of the mean.

toid rocks listed in Table 1 and several groups of ferrodiorites from the NPS; only the monzodiorite group from Umiakovik batholith plots with the ferrodiorites. A substantial compositional gap occurs between the granitoid and ferrodiorite groups for most elements. Rocks of ferrodioritic to monzodioritic composition are shown for comparison only and are not specifically considered in detail in this paper. Note in particular that except for one granitoid group, the silica gap is between 52 and 66 weight % SiO_2. The composition with a K/Ti of 3.5 in Figure 3 represents monzonites from Notakwanon (Table 1), which are likely feldspar-rich cumulates, not representative of liquids. Although intimate physical and chemical mingling and mixing between granitic and ferrodioritic rock compositions have been documented in several NPS intrusions on a small scale by Wiebe and coworkers (Wiebe 1980, Wiebe & Wild 1983), it does not appear that mixing between magmas respectively parental to these two rock types produced large volumes of intermediate compositions. Although responsible for spectacular effects, mixing between granitic and ferrodioritic magmas may, in fact, have been restricted to small volumes. The hyperbolic distributions of Figure 3, although consistent with mixing of two end members, are more likely to reflect processes of crystal–liquid fractionation, particularly within the granitoid compositions.

At present, inadequate sampling precludes estimates of the composition of the pre-NPS crust in the Nain region. Multi-element plots of trace elements in the granitoid rocks are normalized to the composition of post-Archean bulk continental crust (Wedepohl 1991) and shown in Figure 4. The three groupings from bottom to top (north to south in geographic distribution) correspond to greater degrees of fractionation, as indicated by increasingly negative Nb, Sr, Eu, and Ti anomalies and somewhat higher levels of the *REE*. The north-to-south increase in degree of fractionation might be correlated with gradual change in depth of erosion if, as inferred above, the common smaller grain-size and porphyritic textures of Notakwanon rocks reflect shallower depths of crystallization. The granitoid subunits of the Umiakovik batholith show relatively weak fractionation among themselves; the monzodiorite group is chemically distinct, displaying positive Nb and Ti anomalies as well as a much smaller negative Sr anomaly and lower concentrations of the *LREE* (Fig. 4).

Chondrite-normalized *REE* patterns (Fig. 5) in rocks of the Umiakovik batholith display increasing *REE* concentrations and increasingly negative Eu anomalies in the sequence pyroxene monzodiorite, fayalite – pyroxene quartz monzonite, hornblende quartz monzonite and biotite–hornblende granite. The Makhavinekh rocks show a positive Eu anomaly in fayalite facies rocks near the inner anorthositic core, little or no Eu anomaly farther away, and an increasingly negative Eu anomaly far from the core. This distribution would be in accord with a vertically differentiated granitic sheet. The Notakwanon granites have a greater level of *LREE* enrichment than others, coupled with a more strongly negative Eu anomaly. The Voisey Bay granites are more like those of the

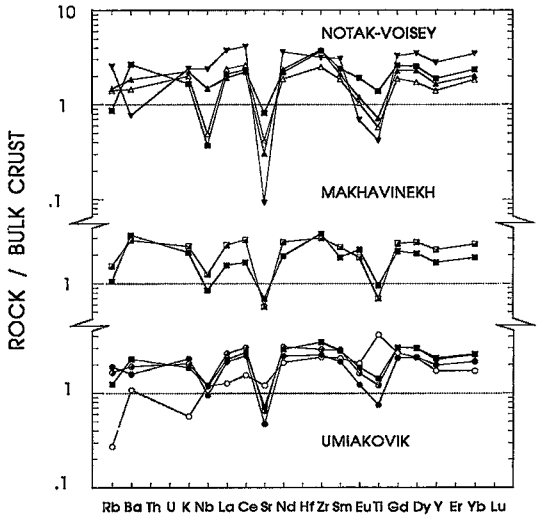

FIG. 4. Extended elemental plots for the principal granitoid masses of the Nain Plutonic Suite. Data from Table 1. Compositions are normalized to the post-Archean bulk crust of Wedepohl (1991).

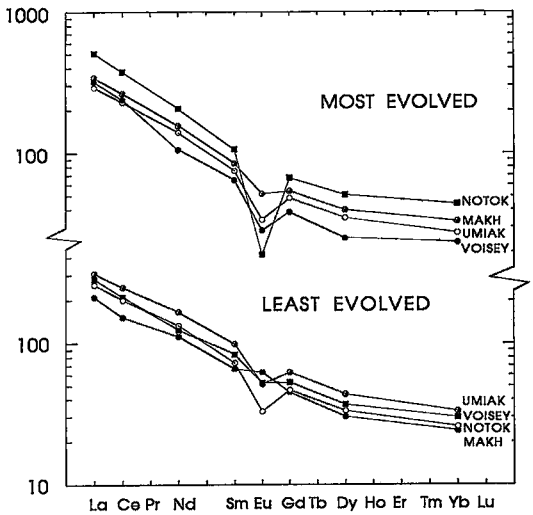

FIG. 5. Chondrite-normalized rare-earth element plots for average compositions of Table 1. Chondrite values from Evensen *et al.* (1978).

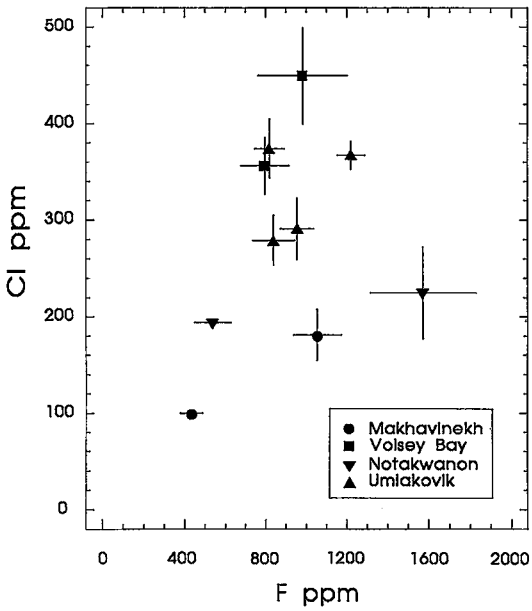

FIG. 6. Weight % chlorine and fluorine in whole rocks.

Makhavinekh pluton than the Notakwanon batholith. The persistent negative Eu anomaly in most granitoids implies that residues of the source materials contained a feldspar (presumably plagioclase) component. The lack of abundant feldspar-rich cumulates among the granitoid compositions argues against the alternative interpretation that early fractionation of feldspar from the magmas caused the negative Eu anomalies.

Concentrations of F and Cl in the whole rocks are plotted in Figure 6. They exhibit a positive correlation. The two groups of Notakwanon samples are relatively low in Cl, unlike biotite and hornblende from the rocks (see below). The Voisey Bay granites, however, are relatively Cl-rich, whereas those from Makhavinekh are lowest in Cl.

Mineral chemistry

Guides to the composition of fluids in equilibrium with the granitoid magmas can be gleaned from the chemistry of such minerals as biotite, hornblende, and apatite. In addition, the Fe–Ti oxide and silicate assemblages place important redox restrictions on the melts and fluids (*e.g.*, Frost *et al.* 1988, Lindsley *et al.* 1990, Lindsley & Frost 1992, Frost & Lindsley 1992). Fluid concentrations and redox conditions are important influences on degrees of partial melting of the sources, rheological properties of the magmas, and the nature of the crystallizing assemblages.

Compositions of selected minerals are presented for samples from the Umiakovik Lake batholith, Makhavinekh pluton, Notakwanon batholith and smaller granite plutons of NPS (Tables 2 to 9, Appendix 1). The distinctive mineral assemblages and mineral chemistry of these middle Proterozoic granites are shown below to be closely correlated with observed and inferred compositions and concentrations of the fluid phase associated with the parental magmas.

Measurement of the concentrations of oxygen was carried out for most samples of biotite and amphibole, and showed good correlation with calcu-

TABLE 2. REPRESENTATIVE COMPOSITIONS OF OLIVINE

	Umiakovik			Makhavinekh			Notakwanon			Voisey
	89-308	89-311	89-324	90-228	90-263	90-264	89-110	89-117	89-119	89-125	90-191
SiO2	30.64	29.63	29.69	29.29	30.16	29.80	29.33	29.33	30.23	29.82	29.01
FeO	68.54	66.16	67.09	66.40	68.24	67.50	68.22	68.36	68.88	68.67	67.01
MnO	1.28	1.06	1.32	0.89	1.32	1.21	1.23	1.07	1.89	1.16	1.30
MgO	1.67	2.11	2.44	1.69	1.21	1.66	1.26	1.34	0.23	0.93	1.79
NiO	0.03	0.04	0.03	0.03	0.01	0.04	0.01	0.04		0.04	0.03
CaO	0.04	0.04	0.03	0.06	0.07	0.07	0.10	0.06	0.07	0.13	0.10
Total	102.20	99.04	100.60	98.36	101.01	100.28	100.15	100.20	101.30	100.75	99.24
O	4	4	4	4	4	4	4	4	4	4	4
Si	1.00	1.00	0.99	1.00	1.00	1.00	0.99	0.99	1.01	1.00	0.98
Fe	1.88	1.86	1.87	1.89	1.90	1.89	1.92	1.92	1.92	1.92	1.90
Mn	0.04	0.03	0.04	0.03	0.04	0.03	0.03	0.03	0.05	0.03	0.04
Mg	0.08	0.11	0.12	0.09	0.06	0.08	0.06	0.07	0.01	0.05	0.09
Ni	0.00	0.00	0.00	0.00	0.00	0.00	0.00	0.00	0.00	0.00	0.00
Ca	0.00	0.00	0.00	0.00	0.00	0.00	0.00	0.00	0.00	0.00	0.00
Total	3.00	3.00	3.02	3.01	3.00	3.00	3.00	3.01	2.99	3.00	3.01
mol%Fa	95.83	94.63	93.92	95.66	96.93	95.79	96.81	96.62	99.40	97.65	95.45
mol%Fo	4.17	5.37	6.08	4.34	3.07	4.21	3.19	3.38	0.60	2.35	4.55

lated stoichiometric O inferred from 24 O – (F+Cl). Both small positive and negative deviations from stoichiometric values occur, suggesting a lack of systematic bias.

Olivine and pyroxenes

Fayalitic olivine is widely distributed in the granitoid rocks of the NPS. It is most abundant in the hornblende- and biotite-poor rocks, but persists as sporadic relict kernels, commonly enclosed by grunerite, in some relatively hornblende- and biotite-rich granitoids. Representative compositions of olivine and the pyroxenes are presented in Tables 2 and 3, respectively.

Ferrous-iron-rich augite is distributed widely, usually in association with fayalitic olivine. Less commonly, ferrosilite and iron-rich pigeonite are present in rocks that bear ferrous-iron-rich augite and fayalite. Pyroxene compositions are plotted in Figure 7, in which comparison is made with pyroxenes from ferrodiorites of the NPS.

Amphibole and biotite

Representative compositions of hornblende are presented in Table 4, and of biotite, in Table 5. The characteristic Fe-rich compositions of hornblende are exhibited in the plot of Fe/(Fe+Mg) *versus* total Al (Fig. 8), and those of biotite, in a plot of Fe/(Fe+Mg) *versus* ^{IV}Al (Fig. 9). Biotite and hornblende from the Notakwanon batholith tend to lie toward the most Fe-rich parts of the range, in accord with indications of more evolved chemistry displayed in Figures 4 and 5.

The composition of biotite and, to a lesser extent, of hornblende displays evidence to support the Fe–F avoidance principle; however, as F decreases with increasing Fe contents, it tends to be replaced by increasing Cl rather than OH (Figs. 10a, b). This

TABLE 3. REPRESENTATIVE COMPOSITIONS AND STRUCTURAL FORMULAE OF PYROXENES

	EC87 -54	EC89 -311	EC90 -228	EC90 -262	EC90 -263	EC89 -110	EC89 -119	EC90 -105	EC90 -108	EC89 -308	EC90 -105	EC90 -219
SiO2	50.25	49.55	47.34	49.31	48.14	48.58	47.79	49.87	48.58	50.74	47.92	49.63
TiO2	0.12	0.23	0.38	0.30	0.23	0.37	0.03	0.15	0.17	0.05	0.12	0.13
Al2O3	0.77	0.74	1.00	1.10	0.74	0.57	0.15	0.62	0.64	0.3	0.25	0.42
Cr2O3	0.03	0.04	0.00	0.03	0.00	0.03	0.00	0.06	0.01	0.02	0.02	0.03
Fe2O3	1.39	0.40	2.20	1.37	2.35	0.39	2.55	1.91	3.90	0.00	0.00	1.10
FeO	19.40	25.01	26.18	25.07	26.14	28.46	27.01	20.30	19.74	42.35	41.91	37.08
MnO	0.31	0.41	0.40	0.39	0.49	0.50	0.52	0.61	0.53	0.61	1.19	0.88
NiO	0.04	0.06	0.00	0.03	0.00	0.01	0.00	0.04	0.05	0.02	0.01	0.01
MgO	7.61	4.41	2.54	3.91	2.54	2.65	0.81	6.42	7.21	5.36	7.13	11.36
CaO	20.51	20.01	19.27	20.36	19.78	18.71	20.81	20.51	18.71	0.60	0.95	0.87
Na2O	0.12	0.09	0.24	0.15	0.26	0.16	0.32	0.23	0.23	0.08	0.01	0.03
K2O	0.01	0.01	0.01	0.00	0.02	0.00	0.01	0.01	0.01	0.01	0.01	0.00
Total	100.56	100.96	99.56	102.02	100.69	100.43	100.00	100.73	99.78	100.15	99.52	101.53
O	6.00	6.00	6.00	6.00	6.00	6.00	6.00	6.00	6.00	6.00	6.00	6.00
SiIV	1.96	1.97	1.94	1.95	1.95	1.98	1.97	1.96	1.93	2.07	1.99	1.97
AlIV	0.04	0.03	0.05	0.05	0.04	0.02	0.01	0.03	0.03	0.00	0.01	0.02
T site	2.00	2.00	1.99	2.00	1.99	2.00	1.98	1.99	1.96	2.07	2.00	1.99
AlVI	0.00	0.01	0.00	0.00	0.00	0.00	0.00	0.00	0.00	0.02	0.01	0.00
Ti	0.00	0.01	0.01	0.01	0.01	0.01	0.00	0.00	0.00	0.00	0.00	0.00
Cr	0.00	0.00	0.00	0.00	0.00	0.00	0.00	0.00	0.00	0.00	0.00	0.00
Fe3+	0.04	0.01	0.07	0.04	0.07	0.01	0.08	0.06	0.12	0.00	0.00	0.03
Fe2+	0.63	0.83	0.90	0.83	0.89	0.97	0.93	0.67	0.66	1.45	1.46	1.23
Mn	0.01	0.01	0.01	0.01	0.02	0.02	0.02	0.02	0.02	0.02	0.04	0.03
Ni	0.00	0.00	0.00	0.00	0.00	0.00	0.00	0.00	0.00	0.00	0.00	0.00
Mg	0.44	0.26	0.15	0.23	0.15	0.16	0.05	0.38	0.43	0.33	0.44	0.67
Ca	0.86	0.85	0.85	0.86	0.86	0.81	0.92	0.86	0.80	0.03	0.04	0.04
Na	0.01	0.01	0.02	0.01	0.02	0.01	0.03	0.02	0.02	0.01	0.00	0.00
K	0.00	0.00	0.00	0.00	0.00	0.00	0.00	0.00	0.00	0.00	0.00	0.00
M1,M2	2.00	2.00	2.01	2.00	2.01	2.00	2.02	2.01	2.04	1.87	2.00	2.01
Fe/Fe+Mg	0.60	0.76	0.86	0.79	0.86	0.86	0.95	0.66	0.64	0.81	0.77	0.65

Note: Fe3+ calculated from stoichiometry and charge balance.

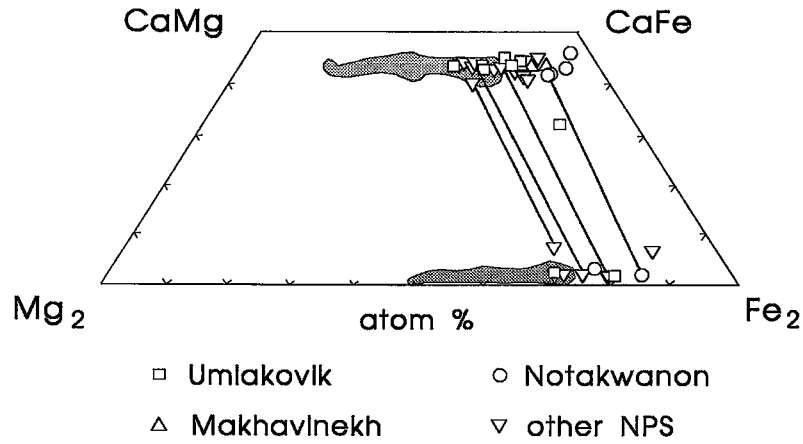

FIG. 7. Pyroxene compositions from NPS granitoids plotted on the quadrilateral. For comparison, shaded areas enclose pyroxene compositions from ferrodiorites widely distributed in the NPS (unpubl. data of R.F.E.). A few tie-lines are shown; the most magnesian pair is from monzodiorite from the Umiakovik batholith.

TABLE 4. REPRESENTATIVE COMPOSITIONS AND STRUCTURAL FORMULAE OF HORNBLENDE

	EC89 -308	EC89 -311	EC90 -253	EC90 -263	EC89 -229	EC89 -110	EC89 -119	EC90 -105	EC90 -108
SiO2	42.10	40.95	39.62	40.05	40.05	41.91	40.45	41.55	40.37
TiO2	1.70	1.95	1.40	1.72	1.23	1.68	1.65	1.85	1.72
Al2O3	8.79	9.15	10.39	8.37	9.62	8.31	6.95	9.20	8.84
Cr2O3	0.00	0.00	0.04	0.00	0.00	0.03	0.00	0.03	0.01
FeO	30.17	28.17	28.46	31.75	31.58	29.99	34.10	27.27	25.74
MnO	0.21	0.23	0.19	0.31	0.45	0.35	0.40	0.30	0.25
MgO	3.52	3.81	3.18	1.92	1.29	3.55	0.60	5.01	5.89
ZnO	0.10	0.10	0.09	0.10	-	0.11	0.21	0.15	0.04
CaO	10.62	10.35	10.82	10.59	10.63	10.30	10.21	10.82	10.79
Na2O	1.56	0.71	1.28	1.64	1.79	1.32	1.79	1.43	1.46
K2O	1.31	1.51	1.60	1.40	1.52	1.28	1.29	1.20	1.47
H2O	1.69	1.48	1.66	1.60	1.63	1.56	1.64	1.77	1.51
F	0.40	0.71	0.40	0.41	0.35	0.60	0.11	0.23	0.58
Cl	0.15	0.21	0.03	0.17	0.19	0.19	0.47	0.11	0.33
O=F	0.17	0.30	0.17	0.17	0.15	0.25	0.05	0.10	0.24
O=Cl	0.03	0.05	0.01	0.04	0.04	0.04	0.11	0.02	0.07
Total	102.12	98.98	98.98	99.82	100.14	100.89	99.71	100.80	98.69
O	22.00	22.00	22.00	22.00	22.00	22.00	22.00	22.00	22.00
SiIV	6.60	6.57	6.40	6.53	6.50	6.65	6.69	6.52	6.47
AlIV	1.40	1.43	1.60	1.47	1.50	1.35	1.31	1.48	1.53
T site	8.00	8.00	8.00	8.00	8.00	8.00	8.00	8.00	8.00
AlVI	0.22	0.30	0.38	0.14	0.34	0.20	0.04	0.22	0.15
Ti	0.20	0.24	0.17	0.21	0.15	0.20	0.21	0.22	0.21
Cr	0.00	0.00	0.01	0.00	.00	0.00	0.00	0.00	0.00
Mg	0.82	0.91	0.77	0.47	0.31	0.84	0.15	1.17	1.41
Fe2+	3.76	3.55	3.68	4.18	4.20	3.75	4.60	3.38	3.24
M1,2,3	5.00	5.00	5.00	5.00	5.00	5.00	5.00	5.00	5.00
Fe2+	0.20	0.24	0.16	0.15	0.08	0.23	0.11	0.20	0.21
Zn	0.01	0.01	0.01	0.01	0.00	0.01	0.03	0.02	0.00
Mn	0.03	0.03	0.03	0.04	0.06	0.05	0.06	0.04	0.03
Ca	1.76	1.72	1.80	1.80	1.85	1.71	1.81	1.75	1.75
M4 site	2.00	2.00	2.00	2.00	2.00	2.00	2.00	2.00	2.00
Ca	0.02	0.06	0.07	0.05	0.00	0.04	0.00	0.07	0.11
Na	0.48	0.22	0.40	0.52	0.56	0.41	0.57	0.43	0.45
K	0.26	0.31	0.33	0.29	0.31	0.26	0.27	0.24	0.30
A site	0.76	0.59	0.80	0.86	0.87	0.70	0.85	0.75	0.86
OH	1.76	1.58	1.79	1.74	1.77	1.65	1.81	1.86	1.62
F	0.20	0.36	0.20	0.21	0.18	0.30	0.06	0.11	0.29
Cl	0.04	0.06	0.01	0.05	0.05	0.05	0.13	0.03	0.09
AlT	1.62	1.73	1.98	1.61	1.84	1.55	1.36	1.70	1.67
Fe/Fe+Mg	0.83	0.81	0.83	0.90	0.93	0.83	0.97	0.75	0.71

Notes: Structural formulae calculated on the basis of 24 O,OH,F,Cl.

TABLE 5. REPRESENTATIVE COMPOSITIONS AND STRUCTURAL FORMULAE OF BIOTITE

	EC89 -324	EC89 -311	EC87 -119	EC87 -152A	EC89 -229	EC90 -187	EC89 -117	EC89 -128	EC90 -106
SiO2	34.79	35.06	33.89	38.38	32.60	33.72	33.35	33.80	34.55
TiO2	3.05	3.39	2.84	0.28	3.77	3.12	3.40	3.29	5.80
Al2O3	12.87	12.85	12.32	22.50	12.81	12.91	11.20	11.90	12.75
Cr2O3	0.01	0.06	0.00	0.01	0.03	0.06	0.00	0.01	0.00
FeO	28.96	29.82	32.38	22.13	34.71	33.63	34.76	37.10	29.51
MnO	0.10	0.08	0.23	0.72	0.27	0.25	0.06	0.15	0.15
MgO	6.67	5.92	4.34	0.18	1.91	2.80	2.84	0.70	4.48
BaO	0.07	0.16	0.13	0.06	0.35	0.39	0.44	0.07	0.28
CaO	0.03	0.03	0.06	0.00	0.15	0.06	0.00	0.00	0.06
Na2O	0.04	0.05	0.07	0.12	0.08	0.05	0.08	0.03	0.16
K2O	9.81	9.01	8.56	10.31	9.02	8.62	9.08	9.43	9.01
H2O	3.23	2.91	3.04	1.81	3.46	3.41	2.96	3.21	3.50
F	1.02	1.70	1.18	4.34	0.18	0.23	0.68	0.25	0.42
Cl	0.03	0.04	0.20	0.07	0.25	0.48	1.15	0.93	0.14
O=F	0.43	0.72	0.50	1.83	0.08	0.10	0.29	0.11	0.18
O=Cl	0.01	0.01	0.05	0.02	0.06	0.11	0.26	0.21	0.03
Total	100.24	100.35	98.69	99.06	99.45	99.52	99.45	100.55	100.60
O	20.00	20.00	20.00	20.00	20.00	20.00	20.00	20.00	20.00
SiIV	5.56	5.60	5.60	5.90	5.44	5.57	5.60	5.64	5.51
AlIV	2.43	2.40	2.40	2.10	2.52	2.43	2.22	2.34	2.40
TiIV	0.01	0.00	0.01	0.00	0.04	0.00	0.18	0.02	0.09
T site	8.00	8.00	8.00	8.00	8.00	8.00	8.00	8.00	8.00
AlVI	0.00	0.02	0.00	1.98	0.00	0.08	0.00	0.00	0.00
TiIV	0.36	0.41	0.35	0.03	0.44	0.39	0.25	0.39	0.60
Cr	0.00	0.01	0.00	0.00	0.00	0.01	0.00	0.00	0.00
Fe2+	3.87	3.98	4.47	2.85	4.85	4.64	4.88	5.18	3.94
Mn2+	0.01	0.01	0.03	0.09	0.04	0.03	0.01	0.02	0.02
Mg	1.59	1.41	1.07	0.04	0.47	0.69	0.71	0.17	1.06
O site	5.84	5.84	5.92	4.99	5.80	5.84	5.85	5.77	5.63
Ba	0.00	0.01	0.01	0.00	0.02	0.03	0.03	0.00	0.02
Ca	0.00	0.00	0.01	0.00	0.03	0.01	0.00	0.00	0.01
Na	0.01	0.02	0.02	0.04	0.03	0.02	0.03	0.01	0.05
K	2.00	1.84	1.80	2.02	1.92	1.82	1.95	2.01	1.83
A site	2.02	1.87	1.84	2.06	2.00	1.87	2.00	2.02	1.91
OH	3.48	3.13	3.33	1.87	3.83	3.75	3.31	3.61	3.75
F	0.52	0.86	0.62	2.11	0.10	0.12	0.36	0.13	0.21
Cl	0.01	0.01	0.06	0.02	0.07	0.13	0.33	0.26	0.04
Fe/Fe+Mg	0.71	0.74	0.81	0.99	0.91	0.87	0.87	0.97	0.79

Notes: Structural formulae calculated on the basis of 24 O,OH,F,Cl.

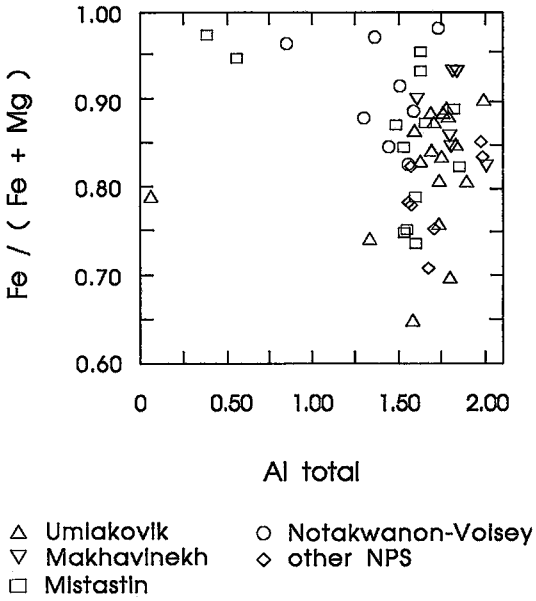

FIG. 8. Fe/(Fe+Mg) *versus* total Al (per 24 O,OH,F,Cl) in hornblende from granitoids of NPS. Samples lowest in Fe/(Fe+Mg) are from dioritic rocks. One sample of grunerite from Umiakovik is plotted (lowest Al, from Appendix 1).

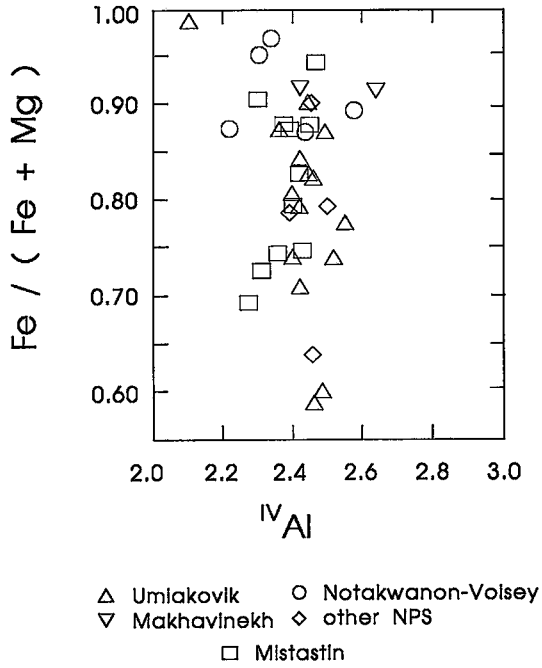

FIG. 9. Fe/(Fe+Mg) *versus* ^{IV}Al (per 24 O,OH,F,Cl) in biotite from granitoids of NPS. Low Fe/(Fe+Mg) samples are from dioritic rocks.

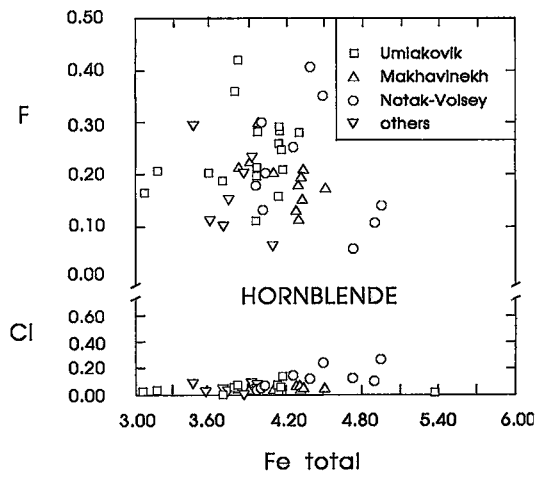

FIG. 10a. Concentration of F and Cl *versus* total Fe in hornblende from NPS granitoids. Fe on the basis of 24 O,OH,F,Cl, and F and Cl on the basis of 2 OH,F,Cl.

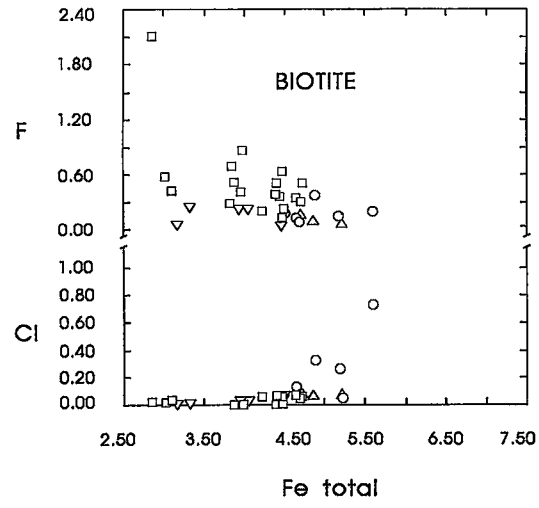

FIG. 10b. Concentrations of F and Cl *versus* total Fe in biotite from NPS granitoids. Fe on the basis of 24 O,OH,F,Cl, and F and Cl on the basis of 4 OH,F,Cl. Symbols as in Fig. 10a.

implies that fluids in equilibrium with the magmas were indeed water-deficient, as supported by other lines of evidence discussed below. The observed relationship in which Cl substitution is preferred by Fe-rich compositions has been discussed by Munoz & Swenson (1981) and Volfinger *et al.* (1985).

The distribution of F and Cl in biotite and hornblende is, for the most part, regular. The plot of wt% F in hornblende *versus* wt% F in biotite (Fig. 11) suggests nonlinear partitioning; at higher levels of F, biotite tends to incorporate F more readily than hornblende, whereas at lower levels of F, the opposite condition applies. A similar effect is indicated for Cl distribution between hornblende and biotite (Fig. 12). The highest levels of Cl are present in biotite and hornblende from the Notakwanon and Voisey Bay – Zoar granites. One pair, with about 0.5 wt% Cl in hornblende and negligible amounts in biotite, is from monzodiorite of the Umiakovik Lake batholith, and seems anomalous. F/Cl ratios in biotite and hornblende are displayed in Figure 13 and clearly suggest partitioning such that F/Cl in biotite increases much more rapidly than F/Cl in hornblende, especially at ratios above about 2. Although biotite and hornblende crystallized together for extended intervals, petrographic evidence indicates that hornblende was more abundant at the earlier stages, and biotite became

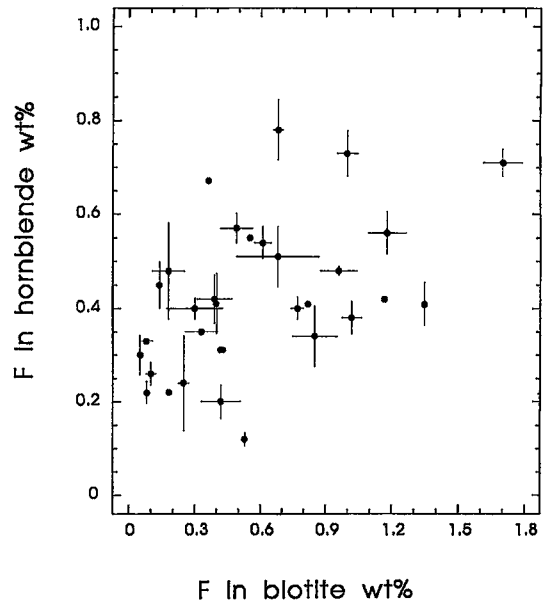

FIG. 11. Wt% F in hornblende *versus* wt% F in coexisting biotite from NPS granitoids. Bars indicate one standard error of the mean for averaged analyses (most are averages of four spot analyses).

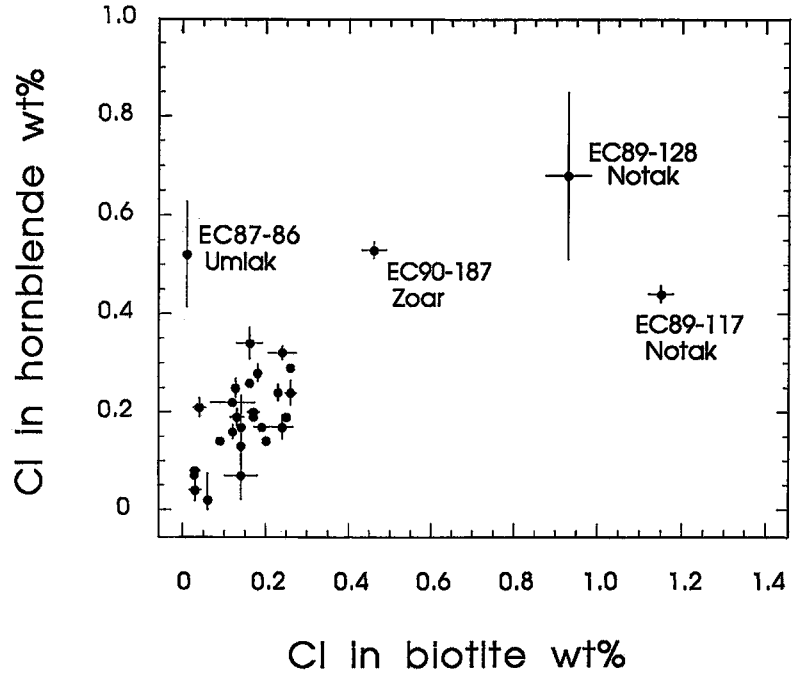

FIG. 12. Wt% Cl in hornblende *versus* wt% Cl in coexisting biotite from NPS granitoids. Bars indicate one standard error of the mean for averaged analyses (most are averages of four spot analyses). Outlying samples are identified.

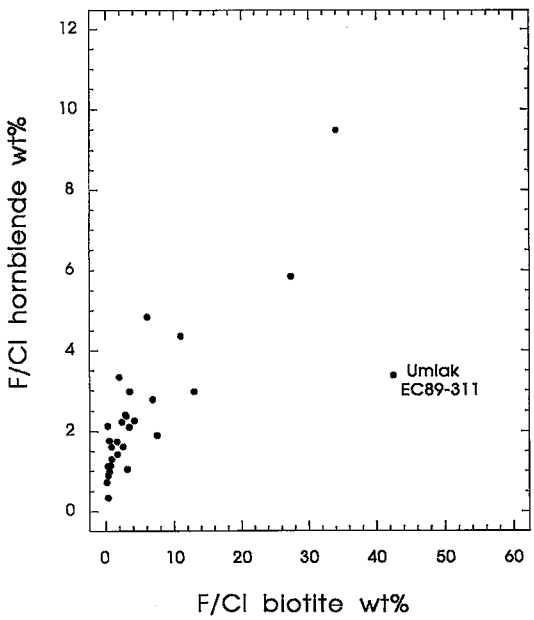

FIG. 13. Wt% F/Cl in hornblende *versus* wt% F/Cl in coexisting biotite from NPS granitoids. One apparently anomalous sample from the Umiakovik batholith is identified.

TABLE 7. REPRESENTATIVE COMPOSITIONS AND STRUCTURAL FORMULAE OF ILMENITE

	Umiakovik			Makhavinek		Notakwanon		Dog Island	
	89-311	90-228	87-119	90-262	90-264	89-110	89-119	90-105	90-108
SiO2	0.00	0.00	0.02	0.00	0.02	0.00	0.00	0.00	0.00
TiO2	50.57	49.89	49.81	51.04	51.48	49.77	50.11	50.57	50.16
Al2O3	0.04	0.04	0.04	0.04	0.06	0.04	0.04	0.04	0.04
Cr2O3	0.09	0.01	0.00	0.03	0.03	0.00	0.00	0.03	0.01
FeO	46.93	47.95	47.21	48.95	47.38	48.29	46.52	48.51	47.84
MnO	0.53	0.46	1.46	0.58	0.85	0.66	1.78	0.81	1.19
MgO	0.05	0.08	0.03	0.08	0.03	0.03	0.02	0.13	0.03
CaO	0.01	0.04	0.03	0.04	0.01	0.03	0.01	0.03	0.01
Total	98.22	98.47	98.60	100.76	99.86	98.82	98.48	100.12	99.28
O	3.00	3.00	3.00	3.00	3.00	3.00	3.00	3.00	3.00
Si	0.00	0.00	0.00	0.00	0.00	0.00	0.00	0.00	0.00
Ti	0.98	0.96	0.96	0.96	0.98	0.95	0.96	0.96	0.95
Al	0.00	0.00	0.00	0.00	0.00	0.00	0.00	0.00	0.00
Cr	0.00	0.00	0.00	0.00	0.00	0.00	0.00	0.00	0.00
Fe3+	0.04	0.08	0.08	0.08	0.04	0.09	0.07	0.09	0.09
Fe2+	0.96	0.94	0.92	0.94	0.96	0.94	0.92	0.93	0.92
Mn	0.01	0.01	0.03	0.01	0.02	0.01	0.04	0.02	0.03
Mg	0.00	0.00	0.00	0.00	0.00	0.00	0.00	0.00	0.01
Ca	0.00	0.00	0.00	0.00	0.00	0.00	0.00	0.00	0.00
Cations	2.00	2.00	2.00	2.00	2.00	2.00	2.00	2.00	2.00
Xhem	0.02	0.04	0.04	0.04	0.04	0.05	0.04	0.04	0.05
Xilm	0.98	0.96	0.96	0.96	0.96	0.95	0.96	0.96	0.95

Note: Fe3+ calculated from charge balance and stoichiometry.

dominant later. The observed differences in F/Cl in the two minerals may relate to progressive concentration of F relative to Cl in more fractionated magmas. One outlying pair in Figure 13 has a very high F/Cl value in biotite; the sample is from the Umiakovik batholith and seems anomalous.

Feldspars

Some rocks contain only perthite, but the more common assemblage consists of plagioclase (oligoclase to andesine) plus perthite. Plagioclase mantles on perthite ovoids in the Makhavinekh pluton consist

TABLE 6. REPRESENTATIVE COMPOSITIONS AND STRUCTURAL FORMULAE OF FELDSPAR

	87-54	89-311	98-311	90-228	90-262	90-262	90-263	90-263	89-110	89-110	89-119	89-119	90-108	90-108
	kspar	plag	kspar	plag	plag	kspar	plag	kspar	plag	kspar	plag	kspar	plag	kspar
SiO2	61.93	59.75	63.60	60.86	58.19	62.38	58.08	61.98	63.02	64.74	66.75	63.20	61.01	60.29
Al2O3	18.01	24.96	18.52	24.64	25.00	18.63	24.28	18.12	22.54	19.06	19.14	17.67	23.67	20.94
FeO	0.08	0.15	1.03	0.24	0.15	0.04	0.21	0.12	0.48	0.18	0.17	0.17	0.26	0.15
CaO	0.29	6.42	0.07	6.44	7.14	0.20	6.60	0.06	4.02	0.35	0.52	0.01	5.36	3.13
Na2O	1.17	7.80	2.36	8.11	7.36	1.32	7.78	1.54	9.11	4.64	11.77	1.56	8.49	5.58
K2O	16.45	0.29	13.73	0.19	0.41	15.56	0.37	14.93	0.48	10.41	0.14	16.66	0.31	6.47
BaO	1.25	0.06	0.52	0.02	0.00	1.18	0.06	0.86	0.21	0.68	0.06	0.22	0.03	0.51
SrO	0.01	0.02	0.01	0.07	0.05	0.06	0.05	0.02	0.00	0.04	0.02	0.01	0.02	0.07
Total	99.19	99.45	99.84	100.57	98.30	99.37	97.43	97.63	99.86	100.10	98.57	99.50	99.15	97.14
n	5	5	4	4	3	5	7	4	3	3	5	4	4	2
Si	11.78	10.72	11.82	10.79	10.59	11.77	10.67	11.84	11.22	11.83	11.90	11.89	10.95	11.29
Al	4.04	5.28	4.06	5.15	5.36	4.14	5.26	4.08	4.73	4.11	4.02	3.92	5.01	4.62
Fe2+	0.01	0.02	0.16	0.04	0.02	0.01	0.03	0.02	0.07	0.03	0.02	0.03	0.04	0.02
Ca	0.06	1.23	0.01	1.22	1.39	0.04	1.30	0.01	0.77	0.07	0.10	0.00	1.03	0.63
Na	0.43	2.71	0.85	2.79	2.60	0.48	2.77	0.57	3.14	1.64	4.07	0.57	2.96	2.03
K	3.99	0.07	3.26	0.04	0.10	3.75	0.09	3.64	0.11	2.43	0.03	4.00	0.07	1.55
Ba	0.09	0.00	0.04	0.00	0.00	0.09	0.00	0.06	0.01	0.05	0.00	0.02	0.00	0.04
Sr	0.00	0.00	0.00	0.01	0.00	0.01	0.01	0.00	0.00	0.00	0.00	0.00	0.00	0.01
Total	20.40	20.03	20.20	20.04	20.06	20.29	20.13	20.22	20.05	20.16	20.14	20.43	20.06	20.19
O	32.00	32.00	32.00	32.00	32.00	32.00	32.00	32.00	32.00	32.00	32.00	32.00	32.00	32.00
mol%Ab	9.64	67.61	20.63	68.78	63.60	11.32	66.63	13.49	78.23	39.71	96.86	12.48	72.83	48.24
mol%Or	89.02	1.65	79.03	1.07	2.33	87.75	2.10	86.23	2.72	58.64	0.78	87.46	1.77	36.79
mol%An	1.34	30.74	0.34	30.15	34.07	0.93	31.26	0.27	19.05	1.66	2.35	0.06	25.40	14.97

Notes: n = number of analyses averaged.

of sodic oligoclase. Representative compositions of feldspars are shown in Table 6.

Ilmenite

Ilmenite is the sole Fe–Ti oxide mineral present in nearly all of the granitoid samples examined. It is also consistently poor in the hematite component. Representative compositions of ilmenite are presented in Table 7.

Apatite

Apatite is one of the most widespread and abundant accessory minerals in the NPS granitoid rocks. Representative compositions are given in Table 8. A plot of concentration of Ce in apatite *versus* that in the host rock (Fig. 14) shows a strong correlation in exponential-like form. Because P_2O_5 generally decreases in more evolved, SiO_2-rich, and Ce-rich granitoid subunits (Table 1), it is inferred that rocks richer in *LREE* contain minerals other than apatite that are rich in *LREE*. This could result if other *LREE*-enriched accessory minerals (allanite? fluorite?) became more common in *LREE*-rich granites or if apatite crystallized in diminished abundance as the *LREE* became concentrated in the more evolved liquids. The implication is that apatite carries a higher proportion of whole-rock *LREE* in less-evolved granitoids than in the more evolved granitoids.

TABLE 8. REPRESENTATIVE COMPOSITIONS AND STRUCTURAL FORMULAE OF APATITE

	Umiakovik						Makhavinekh		Notakwanon		Dog Is.
	89-311	89-323 rims	89-323 cores	89-324	89-325	87-119	89-229 lo-REE	89-229 hi-REE	89-110	89-125	90-179
SiO2	0.45	1.82	1.07	1.39	0.81	2.67	1.11	2.52	1.60	10.65	0.71
FeO	0.08	0.01	0.00	0.00	0.04	0.08	0.06	0.00	0.05	0.00	0.10
MnO	0.03	0.03	0.03	0.03	0.03	0.03	0.03	0.03	0.03	0.09	0.05
CaO	54.46	52.01	53.66	53.20	54.34	51.36	53.17	50.13	52.68	34.29	54.50
SrO	0.07	0.00	0.05	0.00	0.05	0.00	0.02	0.00	0.02	0.00	0.06
P2O5	40.05	37.83	39.23	38.56	39.82	36.09	38.88	36.32	38.04	20.58	39.82
La2O3	0.35	0.84	0.55	0.75	0.41	1.02	0.36	1.31	0.82	5.44	0.43
Ce2O3	0.68	2.01	1.23	1.52	0.94	2.31	0.80	2.78	1.85	11.65	0.91
Nd2O3	0.27	0.90	0.54	0.70	0.47	1.18	0.45	1.25	0.92	4.68	0.41
Sm2O3	0.06	0.20	0.12	0.16	0.12	0.32	0.15	0.32	0.22	1.09	0.09
EuO	0.03	0.06	0.07	0.04	0.03	0.10	0.04	0.10	0.07	0.28	0.06
Gd2O3	0.03	0.16	0.10	0.17	0.12	0.32	0.10	0.29	0.22	0.86	0.10
Dy2O3	0.05	0.11	0.07	0.08	0.08	0.21	0.11	0.15	0.14	0.60	0.05
Er2O3	0.01	0.03	0.00	0.02	0.03	0.02	0.01	0.00	0.02	0.07	0.01
F	3.87	3.52	3.82	3.29	3.82	3.93	3.67	3.86	3.76	2.98	3.34
Cl	0.02	0.01	0.01	0.02	0.01	0.06	0.02	0.01	0.02	0.15	0.05
O=F,Cl	1.63	1.48	1.61	1.39	1.61	1.67	1.55	1.63	1.59	1.29	1.42
Total	98.88	98.06	98.94	98.54	99.51	98.03	97.43	97.44	98.87	92.12	99.27
n	4	7	7	4	12	6	4	4	12	10	13
Si	0.08	0.32	0.19	0.24	0.14	0.48	0.19	0.45	0.28	2.32	0.12
Fe2+	0.01	0.00	0.00	0.00	0.01	0.01	0.01	0.00	0.01	0.00	0.01
Mn	0.01	0.01	0.01	0.01	0.01	0.01	0.01	0.01	0.01	0.02	0.01
Ca	10.06	9.82	9.97	9.94	10.01	9.84	9.98	9.66	9.90	7.99	10.04
Sr	0.01	0.00	0.00	0.00	0.00	0.00	0.00	0.00	0.00	0.00	0.01
P	5.85	5.65	5.76	5.70	5.80	5.46	5.77	5.53	5.65	3.79	5.80
La3+	0.02	0.05	0.04	0.05	0.03	0.07	0.02	0.09	0.05	0.44	0.03
Ce3+	0.04	0.13	0.08	0.10	0.06	0.15	0.05	0.18	0.12	0.93	0.06
Nd3+	0.02	0.06	0.03	0.04	0.03	0.08	0.03	0.08	0.06	0.36	0.03
Sm3+	0.00	0.01	0.01	0.01	0.01	0.02	0.01	0.02	0.01	0.08	0.01
Eu2+	0.00	0.00	0.00	0.00	0.00	0.01	0.00	0.01	0.00	0.02	0.00
Gd3+	0.00	0.01	0.01	0.01	0.01	0.02	0.01	0.02	0.01	0.06	0.01
Dy3+	0.00	0.01	0.00	0.00	0.00	0.01	0.01	0.01	0.01	0.04	0.00
Er3+	0.00	0.00	0.00	0.00	0.00	0.00	0.00	0.00	0.00	0.00	0.00
Total	16.10	16.07	16.10	16.10	16.11	16.16	16.09	16.06	16.11	16.05	16.13
O	25.00	25.00	25.00	25.00	25.00	25.00	25.00	25.00	25.00	25.00	25.00
F	2.11	1.96	2.10	1.82	2.08	2.22	2.03	2.20	2.09	2.05	1.82
Cl	0.01	0.00	0.00	0.01	0.00	0.02	0.01	0.00	0.01	0.06	0.01
OH	0.00	0.03	0.00	0.18	0.00	0.00	0.00	0.00	0.00	0.00	0.17

Notes: Formulae calculated on the basis of 25 O. For sample EC89-229, lo-REE and hi-REE refer to apparent separate populations. Sample EC89-125 may be a member of the britholite series.

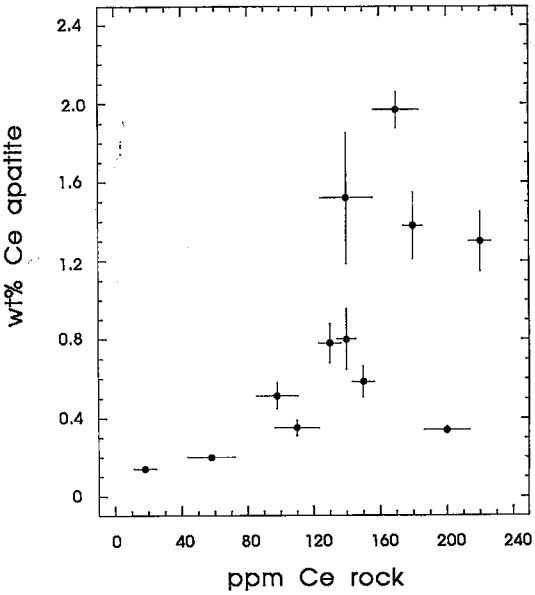

FIG. 14. Wt% Ce in apatite *versus* mean wt% Ce in rock unit (from Table 1). Bars indicate one standard error of the mean.

Apatite from all of the granites approaches fluorapatite; it contains a negligible amount of Cl and only a small amount of OH, a condition that may reflect structural controls (Hughes *et al.* 1989) rather than the composition of the fluid dissolved in the melt (*e.g.*, Boudreau & McCallum 1989). In addition, the F-contents of some samples are unusually high (>3.8 wt%, the concentration in pure fluorapatite), implying either F substitution in other than (OH) sites or a possible analytical problem, such as a change in peak shape between the standard (LiF) and the sample.

Apatite compositions plotted in Figure 15 are consistent with $LREE^{3+}$ coupled with Si^{4+} substituting for (Ca^{2+} + P^{5+}) as described from the Ilímaussaq intrusion by Rønsbo (1989). Sample EC89–125 from the Notokwanon batholith displays an extreme example of this substitution, and may be the mineral britholite.

Intensive variables

Estimates of T, P, $f(H_2O)$, and $f(O_2)$ are possible at different stages of evolution of the granitoid magmas using mineral chemical data, together with some assumptions. It is clear that, for the most part, spot analyses of pyroxene and feldspar compositions represent results of subsolidus equilibration, in accord with coarse grain-sizes and expected slow cooling of the rocks.

Temperatures and pressures

Pressure estimates for the terrane were made by Berg (1977, revised 1979) on contact-metamorphic mineral assemblages over a broad region around and near the NPS. These suggest pressures of 3.5 ± 1 kbar for final crystallization for most or all of the NPS. The southernmost part of NPS, including the Notakwanon batholith, is in large part fine to medium grained and porphyritic (Hill 1982), suggesting it may represent somewhat shallower crystallization than the more northerly bodies.

Petrographic features of most NPS granitoids imply that crystallization took place over a range of temperatures and pressures prior to final emplacement. For example, the assemblage fayalite – augite – quartz occurs widely in all of these granitoid batholiths, whereas fayalite – ferrosilite – quartz is much more restricted. This is consistent with rapid expansion of the Fe-rich pyroxene "forbidden zone" at pressures below about 5 kbar (Lindsley 1983). These Fe-rich olivine- and pyroxene-bearing assemblages are pressure-sensitive (Smith 1971, 1974, Lindsley 1983, Bohlen *et al.* 1980, Koch-Müller *et al.* 1992), but evidence is usually equivocal as to whether the igneous assemblage reached equilibrium at the final level of intrusion rather than at some preceding deeper stage. Using the data of Koch-Müller *et al.* (1992) and assuming temperatures of 700°C for equilibration, maximum pressures in excess of 5.1 kbar are calculated for the Fe-rich olivine – quartz assemblages (higher pressures are calculated if higher temperatures are assumed). Using the same data, orthopyroxene – quartz assemblages indicate minimum pressures ranging from 2.2 to 6.2 kbar; the presence of Ca and sub-

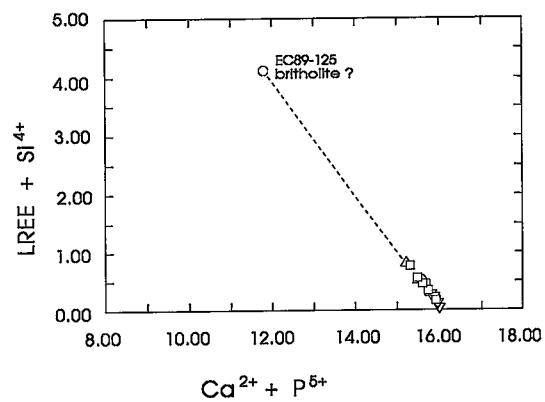

FIG. 15. Plot of *LREE* + Si^{4+} *versus* Ca^{2+} + P^{5+} in apatite from NPS granitoids. All cations on a 25-oxygen basis. The single isolated, collinear sample is EC89–125 from Notakwanon batholith and may be a member of the britholite series. Symbols as in Figure 10a.

stantial Mn in some compositions of orthopyroxene should tend to overestimate pressures. However, temperatures of equilibration for pyroxene- and olivine-bearing assemblages were likely above 700°C, perhaps by 100°C or more, which points to higher pressures of equilibration. Relict equilibrations at higher T and P, reflecting conditions at the source region or during pre-emplacement ponding of magma, cannot be discounted, especially in view of the ubiquitous petrographic evidence that these anhydrous assemblages preceded hornblende- and biotite-bearing assemblages.

Pigeonite (inverted) is common in monzodiorites of the Umiakovik batholith, commonly in association with augite and ferrosilite. Inverted pigeonite also occurs sporadically in fayalite – pyroxene quartz monzonite at Umiakovik, Dog Island and elsewhere. Lindsley (1983) estimated 825°C as the lowest temperature of stability of pigeonite; this temperature can be lowered slightly by the Mn that is present in the pyroxene, but is raised by about 8.5°C per kbar. These latter effects tend to cancel each other in the NPS granitoids, implying that temperatures of at least 825°C applied to the earlier history of crystallization of the NPS granitoid magmas.

A test of the estimated regional pressures of crystallization was attempted using hornblende geobarometry (for a recent assessment, see Ghent *et al.* 1991). The required assemblage of hornblende, plagioclase, K-feldspar, quartz, biotite, magnetite, and titanite is not widely developed. Titanite and magnetite are lacking from most assemblages, as has been noted previously, but are present in a few, and the equivalent Fe-rich augite (or Fe-rich hornblende) plus ilmenite assemblages are common (*e.g.*, Wones 1989):

$$3CaTiSiO_5 + 2Fe_3O_4 + 3SiO_2 = 3CaFeSi_2O_6 + 3FeTiO_3 + O_2$$

$$CaTiSiO_5 + Fe_2SiO_4 = CaFeSi_2O_6 + FeTiO_3$$

$$12\ CaTiSiO_5 + 14Fe_3O_4 + 36SiO_2 + 6H_2O = 6Ca_2Fe_5Si_8O_{22}(OH)_2 + 12FeTiO_3 + 7O_2$$

The hedenbergite- and ilmenite-bearing assemblages are stable only at more reducing or higher temperature conditions than the titanite-bearing assemblages.

Pressure estimates are listed in Table 9 and are in reasonable agreement with the previous estimates from contact metamorphic assemblages. The range of Al_{total} from 1.49 to 1.79 atoms per formula unit amounts to a pressure interval of 2.8 to 4.1 kbar according to equation P1, and 3.6 to 5.3 kbar using equation P2 in Table 9. The relatively small variation of total Al among the hornblende compositions in NPS granitoid rocks supports the interpretation that crystallization pressures did not greatly differ from about 3.5 kbar. The pressure estimates in Table 9 suggest a small but possibly significant decrease in pressure from northern to southern intrusions, consistent with other evidence for a higher level of emplacement to the south.

TABLE 9. APPLICATION OF HORNBLENDE GEOBAROMETERS

Unit or pluton	Altotal xbar	Altotal s.e.	kbar P1	kbar P2
Umiakovik - fay px qtz monz, n=6	1.667	0.075	3.6	4.6
- hb qtz monz, n=4	1.785	0.016	4.1	5.3
- bi hb granite, n=4	1.683	0.036	3.7	4.7
- grand mean, n=14	1.705	0.035	3.8	4.8
Makhavinekh, n=9	1.792	0.035	4.1	5.3
Voisey Bay, n=4	1.528	0.033	3.0	3.8
Notakwanon, n=5	1.489	0.087	2.8	3.6
Dog Island, n=4	1.625	0.036	3.4	4.4

s.e.- one standard error of the mean.

P1(±0.5 kbar) = -3.46(±0.24) + 4.23(±0.13)Al^T (Johnson & Rutherford 1989)

P2(±1 kbar) = -4.76 + 5.64Al^T (Hollister et al.1987)

FLUIDS

Oxygen fugacities

Ilmenite is the sole Fe–Ti oxide mineral in the majority of the granitoid rocks from all of the intrusions considered here. Occurrences of magnetite–ilmenite lamellar intergrowths and of titanite are extremely rare. It is permissible, therefore, to infer that cooling of magmas generally followed $f(O_2)$–T paths defined by the compositions of crystallizing ilmenite (Fig. 16). Hematite contents of ilmenite are consistently low, mostly in the range 2.5 to 4.5 mol%. Subhedral to euhedral platy and rod-like grains of ilmenite occur in all rock types. We infer that ilmenite began to crystallize at an early stage. Application of QUILF and related equilibria (Lindsley *et al.* 1990, Lindsley & Frost 1992) permits calculation of $f(O_2)$–T relations for ilmenite in the assemblages; these are for the most part in the range 1 to 3 log $f(O_2)$ units below FMQ buffer.

Also plotted in Figure 16 are intersections of biotite and ilmenite isopleths in T–$f(O_2)$ space. Note that ilmenite with a low hematite content, like that encountered here, has a trajectory subparallel to FMQ over a substantial range in temperature. Calculated trajectories of biotite assume that $f(H_2O)$ remains equivalent to water saturation in minimum-melt granite compositions as temperature changes; other data on mineral

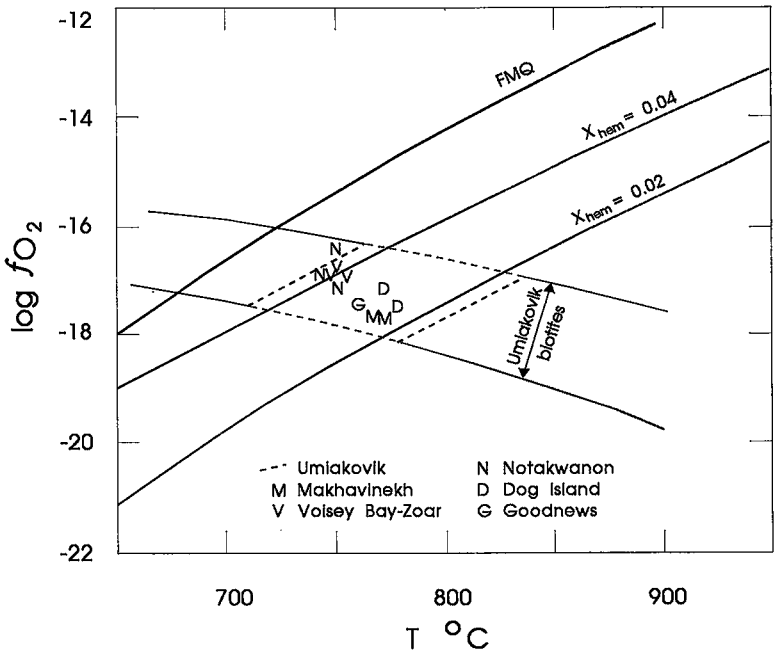

FIG. 16. Plot of log $f(O_2)$ *versus* T°C for NPS granitoid assemblages. Curves labeled X_{hem} = 0.02 and 0.04 refer to ilmenite with 0.02 and 0.04 mol % hematite in solid solution and are subparallel to the FMQ buffer in this temperature range. For the Umiakovik batholith, the observed range of biotite compositions is indicated. Letters indicate individual samples. Calculated for total pressure of 3500 bars.

TABLE 10. MINERAL COMPOSITIONS USED TO CALCULATE EQUILIBRIA

	$(XFe2+)^3.(XOH)^2$	Xmt	XOr	Xfa
Umiakovik				
EC87-54	0.109	0.336	0.890	-
EC87-86	0.172	-	(0.800)	0.968
EC89-302	0.090	-	0.671	0.918
EC89-308	0.171	0.309	(0.800)	0.958
EC89-311	0.116	0.295	0.707	0.946
EC89-323	0.265	0.350	(0.800)	-
EC89-324	0.157	-	0.841	0.939
EC89-342	0.285	0.229	0.796	-
EC87-106	0.288	0.255	0.931	-
EC87-119	0.214	0.599	(0.931)	-
Makhavinekh				
EC89-226	0.344	0.295	0.739	-
EC89-229	0.330	(0.295)	0.927	-
Voisey Bay-Zoar				
EC90-187	0.323	0.482	(0.800)	-
EC90-190	0.339	0.512	0.716	-
EC90-191	0.310	0.635	0.611	0.954
Notakwanon				
EC89-125	0.189	0.638	0.694	0.976
EC89-117	0.263	0.527	0.663	0.966
EC89-128	0.270	0.467	(0.690)	-
Dog Is., etc.				
EC90-106	0.226	0.393	0.774	-
EC90-179	0.231	0.309	(0.800)	-
EC90-181	0.348	0.350	(0.800)	-

Note: Values in brackets are estimated as discussed in the text.

compositions (Table 10) were the same as used for calculation of water fugacities from equation 1(a) in the next section. The assumption of water saturation as a limit is deemed reasonable in view of lack of field evidence for presence of excess water in any of the granitoid magmas (general lack of pegmatites, aplites, miarolitic cavities). The Umiakovik batholith is the largest NPS granitoid intrusion with the greatest compositional range, which helps to account for its substantial range in T–$f(O_2)$ space. Monzodiorites from Umiakovik lie toward the higher-temperature, lower-$f(O_2)$ part of the field, as might be expected.

Water fugacities

Estimates of H_2O fugacities in equilibrium with the magmas can be made by employing biotite equilibria (*e.g.*, Wones & Eugster 1965, Wones 1981). Rigorous application of such equilibria is hampered in NPS rocks because, in general, biotite crystallized late, and it is not always clear whether growth was supersolidus or subsolidus. In particular, biotite occurring in delicate sprays and as fringes on ilmenite, for example, almost certainly grew near or below the solidus. Most rocks contain interstitial to poikilitic biotite, and it is assumed that growth occurred in the presence of liquid near the solidus.

Two equilibria involving biotite were used to estimate water fugacities in the granitoid rocks:

$$KFe_3AlSi_3O_{10}(OH)_2 + 1/2\ O_2 = KAlSi_3O_8 + Fe_3O_4 + H_2O \quad (1)$$

$$\log f(H_2O) = 4819/T(K) + 6.69 - 0.011(P-1)/T(K) + \log a_{Ann} + 1/2 \log f(O_2) - \log a_{Or} - \log a_{Mt} \quad (1a)$$

$$KFe_3AlSi_3O_{10}(OH)_2 + 3/2\ SiO_2 = KAlSi_3O_8 + 3/2\ Fe_2SiO_4 + H_2O \quad (2)$$

$$\log f(H_2O) = -7402/T(K) + 10.84 + 0.036(P-1)/T(K) + \log a_{Ann} + 3/2 \log a_{SiO2} - \log a_{Or} - 3/2 \log a_{Fa} \quad (2a)$$

It is apparent that equilibrium (2) is simply the sum of equilibrium (1) minus one-half the FMQ oxygen buffer equilibrium 3 fayalite = magnetite + 3 quartz. The equilibrium constant (log K) employed in (2a) was calculated by subtracting 1/2 log K for FMQ (Myers & Eugster 1983) from log K for (1a):

$$3/2\ Fe_2SiO_4 + 1/2\ O_2 = Fe_3O_4 + 3/2\ SiO_2 \quad (1/2\ FMQ)$$
$$1/2 \log f(O_2) = 1/2 \log K = -12221/T(K) + 4.145 + 0.047(P-1)/T(K)$$

Problems that arise in evaluating these equilibria include an appropriate expression to describe the activity of annite in biotite, which remains elusive (see Appendix 3 for activity models employed). For present purposes, a_{Ann} is defined as $(XFe^{2+})^3 \cdot (XOH)^2$ as proposed by Czamanske & Wones (1973); F and Cl are low in most examples of Fe-rich biotite in the NPS, so that the *X*OH term remains close to 1. The biotite compositions typically are relatively high in Ti, which is known to extend the upper-temperature stability limits (Hewitt & Wones 1984). All of the K-feldspar in the rocks is perthitic, and the appropriate composition (bulk or exsolved) that was in equilibrium with biotite is problematic; fortunately, most compositions lie in the X_{Or} range of 0.70 to 0.90. Using an estimated value of 0.80 does not change calculated $f(H_2O)$ by more than 0.1–0.2 log units. Magnetite is absent from nearly all rocks, but an appropriate composition that would have been in equilibrium with the ilmenite analyzed was obtained using the QUILF equilibria (Lindsley *et al.* 1990, Lindsley & Frost 1992); a spinel composition thus obtained has a maximum X_{Mt} content.

Equilibrium (1a), the relationship suggested by Wones (1981) for more reduced assemblages (NNO to WM), results in water fugacity estimates of 250 to 550 bars at the water-saturated solidus (Fig. 17). These should be regarded as upper limits for reasons given above. It should also be remembered that these conditions apply only to the later stages of crystallization of the larger granitic intrusions, once biotite became stable.

Equilibrium (2a) delivers consistently slightly higher values of $f(H_2O)$, (900 bars at 710°C to 700 bars at 740°C on the water-saturated solidus) than equilibrium (1a) using the same activity models for biotite and K-feldspar and olivine, as indicated in Appendix 3). The relatively small differences may result from lack of internal consistency in thermodynamic values used for the two equilibria or to the activity model used for magnetite. An alternative is that fayalitic olivine was never stable at lower temperatures near the solidus but only at higher temperatures. Olivine is relatively rare in the NPS biotite – hornblende granitoid rock assemblages, occurring as relict kernels surrounded by grunerite and hornblende shells.

A projection of mean compositions of the granitoids in terms of normative components Q, ab and or is shown in Figure 18. Superimposed are paths of minimum-melt compositions over a range of total pressure and varying $a(H_2O)$ in the melt (data from Ebadi & Johannes 1991). Most compositions tend to cluster at positions consistent with low activities of water and moderate total pressures. The low-Q unit from the Umiakovik batholith is monzodiorite, and that from the Notokwanon batholith is monzonite (unit 16b, Table 1); neither is relevant to data on granitic melts.

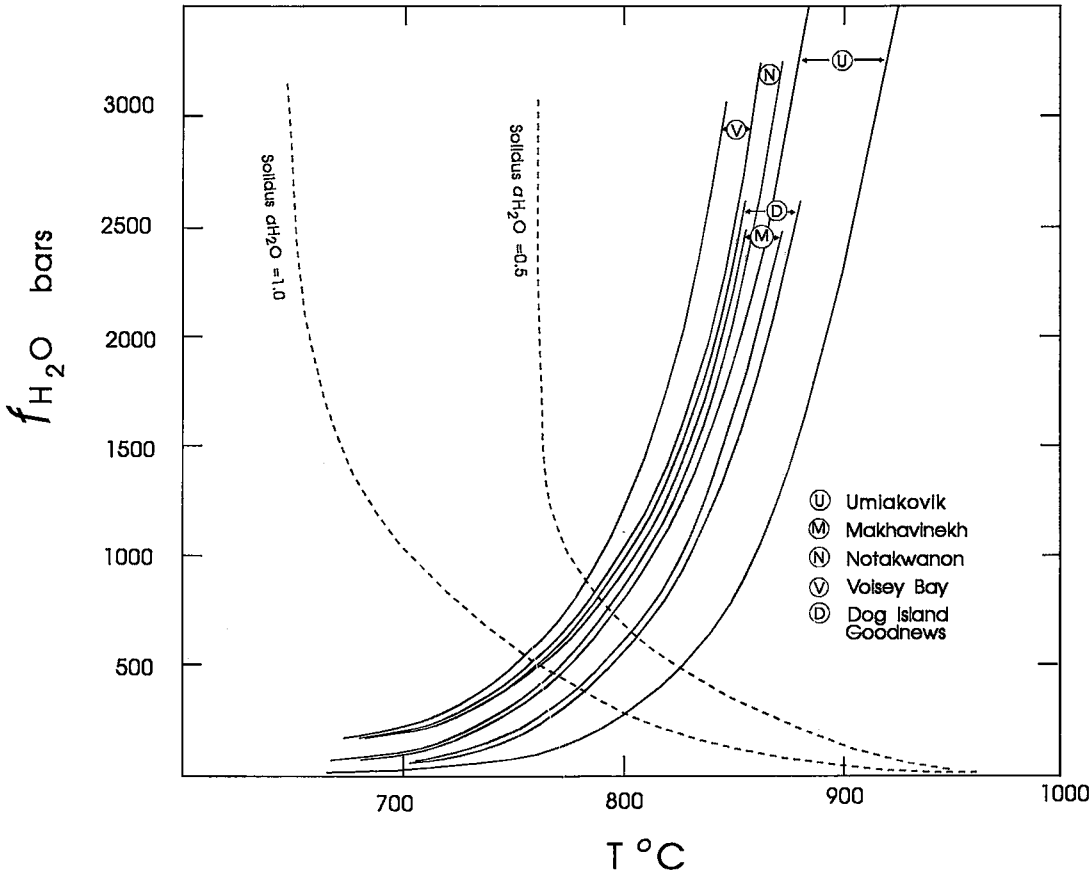

FIG. 17. Plot of $f(H_2O)$ *versus* T°C showing calculated stabilities of biotite for NPS granitoids. Solidi for haplogranite system at $a(H_2O)$ = 1.0 and $a(H_2O)$ = 0.5 from Ebadi & Johannes (1991). Conversions to $f(H_2O)$ were made with the tables of Burnham *et al.* (1969).

Other fluid components

In addition to water, F and, to a much lesser extent, Cl, constituted part of the dissolved fluids in the granitoid magmas. S and CO_2 also were present in small and varying amounts (Table 1). The calculation of water fugacities in the previous section assumes that the proportion of components other than H_2O in the fluids was small enough to ignore.

The extent to which measured proportions of F, Cl, and OH in hydroxyl sites of appropriate minerals retain the state of equilibration with a dissolved magmatic fluid is questionable. Although a measure of regularity exists in F and Cl partitioning between biotite and amphibole, apatite is invariably almost Cl- and OH-free, suggesting that structural constraints operating during subsolidus cooling may have exercised a dominant role in determining its final composition (Hughes *et al.* 1989).

DISCUSSION

The granitoid rocks considered in this study confirm the essential "bimodal" nature of NPS magmatism. The principal rock-type of intermediate composition present in the NPS is ferrodiorite (and monzodiorite), and although mixing and mingling of ferrodiorite and granitic magmas have been well documented by Wiebe (1980) and Wiebe & Wild (1983), there is little indication that substantial volumes of mixed magmas ever formed.

REE and multi-element plots suggest that extreme fractionation of these granitoid magmas did not occur, probably as a result of higher viscosities in water-undersaturated magmas. Indicated ranges of late-stage temperature between about 825°C to 725°C are also in accord with crystallization from water-undersaturated magmas.

Any model for crystallization and cooling of the

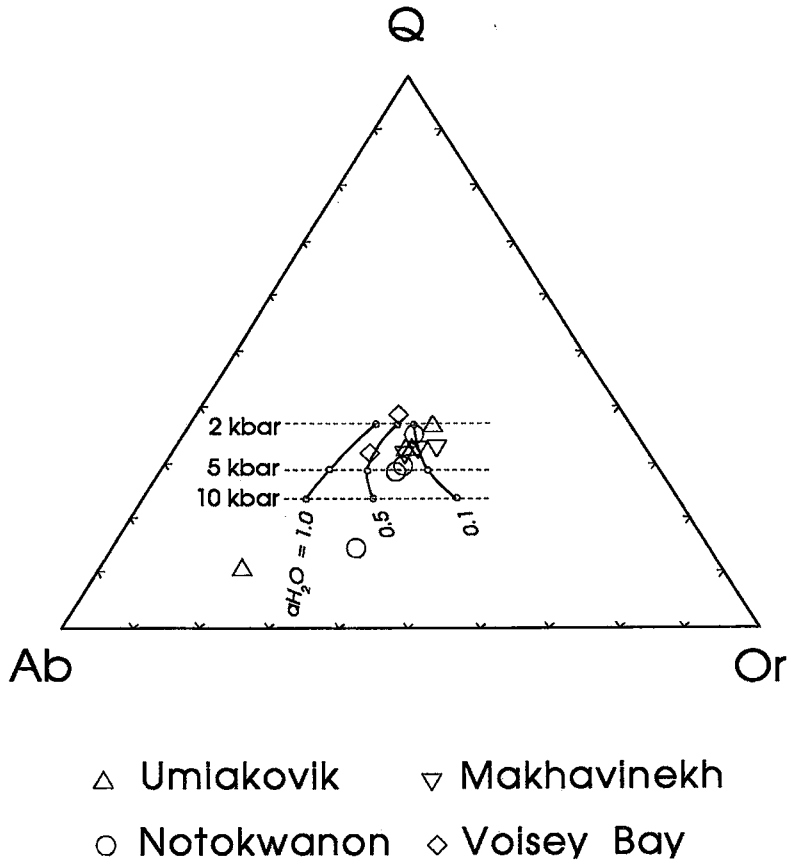

FIG. 18. Granitoid compositions from Table 1 projected in terms of normative Q–ab–or. Also shown are loci of minimum melt compositions with changing total pressure and changing water activities in the melt (from data of Ebadi & Johannes 1991).

NPS granitoids should consider potential heat flow from contemporaneous associated anorthosite and other basic rocks that in many places in the Nain Plutonic Suite underlie or adjoin the granitoids (Figs. 1, 2). Several features may relate to such an association: 1) quartz-poor or quartz-free monzonite (mangerite) tends to occur in the lower parts of the sheets of granitoid rock, adjacent to anorthositic rocks; 2) fluid-poor earlier-crystallized granitoids (more abundant olivine and pyroxenes) occur closer to contacts with anorthosite; 3) later-crystallized, and relatively fluid-enriched, granitoids (more abundant hornblende and biotite) are more distant from contacts with anorthosite, and 4) there is a sporadic presence of the mantled (rapakivi) texture, which has been related, in part, to unusually slow rates of cooling during crystallization (*e.g.*, Nekvasil 1991).

The first two features may reflect gravitational accumulation of crystals or a kind of zone-refining process driven or aided by underlying hot anorthositic and related basic rocks. Such processes could help account for chemical and physical characteristics of feldspar-rich monzonitic fractions, including their depletion in incompatible elements and the common occurrence of resorption-like features on feldspars and quartz in rapakivi granites (see review by Emslie 1991). With a thermal gradient superimposed on the magma, liquid-rich fractions would be expected to migrate more efficiently away from earlier-crystallized material, as may have been the case for the Umiakovik batholith and the Makhavinekh pluton.

Classic rapakivi granite suites that exhibit abundant mantling of perthite ovoids by plagioclase, such as in the Wiborg batholith in Finland, and parts of the Korosten complex in the Ukraine, are closely associated with and, at least partly, underlain by anorthositic rocks. This is also the case for the Makhavinekh pluton, has been suggested by Hill (1982) for the Notakwanon batholith, and may also apply to the Mistastin batholith (Fig. 1). An obvious question is

whether an underlying hot anorthosite pluton may have played a significant role in the development of the mantled texture through modification of normal processes of crystallization and cooling. Rounded, embayed margins of perthite ovoids are commonly described (Emslie 1991), suggesting resorption that could relate to reheating of the magma. Similarly, rounded, drop-like quartz grains and quartz textures of more than one generation are features that could readily be related to reheating that caused local or temporary intervals of resorption.

Several lines of evidence suggest that decompression of water-undersaturated magmas during ascent in the crust, with minimum loss of heat, can lead to development of the mantled textures [for recent views, see Nekvasil (1991) and Emslie (1991)]. As noted, field evidence suggests that substantial plutons of anorthositic rock may underlie many of these batholiths, and possibly accompanied their ascent in the crust. Residual heat from crystallization and cooling of the anorthositic plutons thus may have played a vital role in sustaining the necessary low rate of heat loss from the granitic magma over a protracted period. This would alleviate or remove the requirement to conserve heat by rapid ascent, as proposed by Nekvasil (1991). Such a heat-conserving model could have important implications for understanding how concentration of ore minerals may be facilitated by extending the duration of the crystallization interval, thus enhancing diffusion processes that concentrate incompatible elements such as W, Nb, Sn, Mo in late melts or ore-forming fluids.

Of the NPS granitoid rocks considered here, there is no clear geochemical reason why plagioclase-mantled ovoids should be a prominent feature of the Makhavinekh pluton and be rare or absent in the others. Consideration of mineral equilibria, including estimates of T, $f(O_2)$ and $f(H_2O)$, also offers no ready explanation. It is likely that physical parameters and processes played a crucial role, *e.g.*, rate of decompression during upward transport in the crust, rate of heat loss during transport or subsequent crystallization (Nekvasil 1991).

Extraction of granitoid magmas like those of the NPS from a crustal source implies that residues with specific characteristics remained behind. Such hot residues must be considered as prime potential sources for the contamination for basic magmas associated with the Nain Plutonic Suite.

An important characteristic of the crustal residue is presence of plagioclase (negative Eu anomalies in NPS granitoid rocks) and therefore enrichment in those elements compatible with plagioclase. The residues should be depleted in Rb, Ba, and K and have a low K/Ti value, because a high K/Ti value characterizes the NPS granitoid magmas. Pyroxenes are presumably also important in the residues, which can be characterized petrographically as pyroxene –plagioclase granulites with a positive Eu anomaly. Similar residues are believed to be formed by dehydration partial melting of post-Archean lower crust (*e.g.*, Rudnick 1992). Many of the characteristics that apply to the residues of dehydration partial melting of the crust are embodied in the required characteristics of parental magmas for anorthosites, and such residues must be regarded as superior candidates for contaminants of basaltic magmas to produce anorthositic parental magmas.

This hypothesis conflicts with that of Morse & Hamilton (1991), who argued against crustal contamination of parental magmas to anorthosites on the grounds that bulk crust, or minimum melt derived therefrom, contains too much Rb to permit the very low Rb observed in most anorthositic rocks. However, in view of the potential for crustal partial melting, large-scale contamination of mantle-derived magmas by bulk crust is probably in general an uncommon process. A preceding episode of partial melting of the crust that removed most Rb, Ba, K (and other incompatible elements) into granitoid melts and enriched the remaining residue in Sr and Eu (in plagioclase) would create in the latter residue a most salutary contaminant for production of anorthositic magmas from mantle-derived basaltic magma. The process would be very energy-efficient if the basic magma that caused crustal partial melting subsequently assimilated (by assimilation – fractional crystallization processes) the already heated residue. Recent recognition that some granitoid rocks are older than some basic members of NPS (Emslie & Loveridge 1992) lends support to that kind of model. Recently published isotopic data for anorthositic and related rocks of NPS (Ashwal *et al.* 1988, Emslie & Thériault 1991, Hamilton & Shirey 1992) clearly imply that a significant crustal contribution was present in their parental magmas.

Assuming a bulk post-Archean crust (Wedepohl 1991) as a model source, a maximum of about 48% of average NPS granite can be extracted from it before K is exhausted, but the trace elements Zr, Y, and *LREE* begin to be exhausted after about 35% extraction (Table 1, Fig. 19). This would leave a crustal residue lower in SiO_2, much lower in K, Rb, Ba, Zr, Pb, U, *REE* (especially *LREE*) and enriched in components compatible in intermediate plagioclase and pyroxenes, including Ca, Al, Mg, Sr, Eu, and Ti. Residues like this, at temperatures of 900°C or higher, would be readily assimilated (accompanied by fractional crystallization) by mantle-derived basaltic magma. Assimilation of such residues in quantity by basaltic magma could maintain plagioclase on the liquidus for protracted periods, assisting in development of substantial volumes of anorthositic magma (*i.e.*, plagioclase crystals plus melt). Such a process removes objections raised by Morse & Hamilton (1991) against crustal contamination as a viable process in the gene-

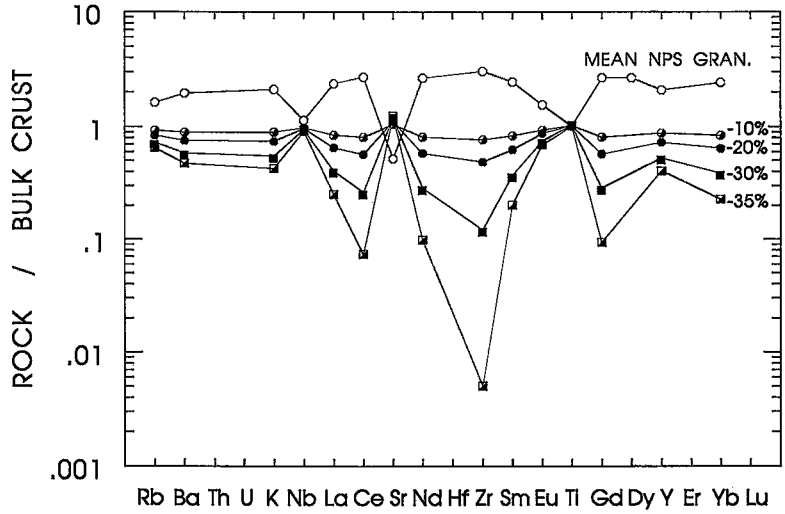

FIG. 19. Extended elemental plot of NPS grand mean granitoid composition ($n = 97$) from Table 1, normalized to post-Archean bulk crust (Wedepohl 1991). Percentages refer to residues remaining after that increment of grand mean NPS granitoid composition has been subtracted from bulk crust.

sis of massif anorthosites. Different degrees of efficiency of separation of partial melt from residue would be unavoidable and could readily explain variations in trace-element signatures within and between anorthosite massifs. As argued by Tsvetkov & Sukhanov (1991), there is little reason to believe that large quantities of anorthositic liquids can be derived directly from the mantle. The model outlined here (see also Emslie & Hegner 1993) regards anorthositic parent magmas as hybrids of mantle and crustal components instead of invoking unusual sources in the mantle to produce Al–Fe basic magmas, as discussed by Olsen & Morse (1990). The present model has components contained in the proposed origin of massif anorthosite by Taylor *et al.* (1984), but emphasizes the required mantle contribution ignored by those authors.

The proposed model may also go some way toward resolving a recent dispute about plagioclase–melt partitioning in the Kiglapait intrusion (Morse 1992, Blundy & Wood 1992), which forms part of the NPS (Fig. 1). If the high-Al character of the parent magma of Kiglapait resulted from assimilation of plagioclase-rich (and Sr-rich) residues from prior partial melting of the crust, excess Sr in the cumulates might be explained without appeal to liquid losses during crystallization of the intrusion and without impugning the validity of the experimental data-base.

SUMMARY AND CONCLUSIONS

The principal granitoid batholiths of the Nain Plutonic Suite have similar ranges of average composition and have fractionated in similar ways, but only to relatively modest extents. Mineral assemblages and biotite equilibria, as well as lack of development of pegmatite and aplite, point to water-undersaturation in even the most fractionated subunits. Water-poor magmas were probably a contributing factor in hampering stronger fractionation because of their increased viscosities.

Indicated ranges of temperature for the later stages of crystallization of NPS granitoids were near 750°–780°C at water fugacities of 250 to 500 bars, and average total pressures about 3.5 kbar. If late-stage activity of water in the magmas was as low as 0.5, this would raise temperature and water fugacity estimates to 780°–825°C, 500 to 900 bars. The indicated minimum range of temperature for the Umiakovik batholith was about 725°–825°C. The Notakwanon and Voisey Bay granites were at the higher-$f(H_2O)$, lower-T part of that range, whereas the Makhavinekh pluton occupied an intermediate position.

Biotite and ilmenite compositions indicate that log $f(O_2)$ was 1 to 3 units below the FMQ buffer at temperature ranges similar to those above. The Notakwanon and Voisey Bay granites lie at the more oxidized part of the range.

Known contemporaneity of basic and silicic magmatism and high degrees of partial melting of the crust are consistent with the formation of large volumes of water-poor, high-temperature granitoid magmas. In the anorogenic setting of the Nain Plutonic Suite, basic magmas were the principal thermal source to

induce partial melting of the crust, and therefore were susceptible to contamination by both melts and residues of the crustal partial melting process. Hot, proximal, plagioclase-rich residues of the partial melting process are highly attractive contaminants to produce anorthositic magmas from basaltic magmas. Consideration of the chemistry of anorthositic rocks reported from NPS [(low concentrations of K, Rb, Zr, and other incompatible elements, high concentrations of Sr, Eu and elements compatible in plagioclase, *e.g.*, Wiebe 1978)] implies that such residue components must generally have been efficiently separated from the melt fraction.

Acknowledgements

The authors are indebted to Deborah Lemkow for careful preparation of the figures and to Gordon Pringle for help in deconvolution of REE spectra during electron-microprobe analysis of apatite. Reviews by B. Bonin, R.F. Martin, W.D. Sinclair and two anonymous referees resulted in significant improvements in presentation and are gratefully acknowledged.

References

Anderson, J.L. (1980): Mineral equilibria and crystallization conditions in the Late Precambrian Wolf River rapakivi massif, Wisconsin. *Am. J. Sci.* **280**, 289-332.

Ashwal, L.D., Wooden, J.L., Wiebe, R.A. & Emslie, R.F. (1988): Isotopic signatures of Proterozoic intrusives in the eastern Canadian Shield as probes to older basement types. *Geol. Assoc. Can. – Mineral. Assoc. Can., Program Abstr.* **13**, 3.

Berg, J.H. (1977): Regional geobarometry in the contact aureoles of the anorthositic Nain complex, Labrador. *J. Petrol.* **18**, 399-430.

——— (1979): Physical constraints and tectonic setting of the Nain complex. *Geol. Assoc. Can. – Mineral. Assoc. Can., Program Abstr.* **4**, 39.

Blundy, J.D. & Wood, B.J. (1992): Partitioning of strontium between plagioclase and melt: reply to a comment by S.A. Morse. *Geochim. Cosmochim. Acta* **56**, 1739-1741.

Bohlen, S.R., Essene, E.J. & Boettcher, A.L. (1980): Reinvestigation and application of olivine – quartz – orthopyroxene barometry. *Earth Planet. Sci. Lett.* **47**, 1-10.

Boudreau, A.E. & McCallum, I.S. (1989): Investigations of the Stillwater Complex. V. Apatites as indicators of evolving fluid composition. *Contrib. Mineral. Petrol.* **102**, 138-153.

Bridgwater, D. & Windley, B.F. (1973): Anorthosites, post-orogenic granites, acid volcanic rocks and crustal development in the North Atlantic Shield during the mid-Proterozoic. *Geol. Soc. S. Afr., Spec. Publ.* **3**, 307-317.

Burnham, C.W., Holloway, J.R. & Davis, N.F. (1969): Thermodynamic properties of water to 1000°C and 10,000 bars. *Geol. Soc. Am., Spec. Pap.* **132**.

Clemens, J.D., Holloway, J.R. & White, A.J.R. (1986): Origin of an A-type granite: experimental constraints. *Am. Mineral.* **71**, 317-324.

Czamanske, G.K. & Wones, D.R. (1973): Oxidation during magmatic differentiation, Finnmarka Complex, Oslo area, Norway. 2. The mafic silicates. *J. Petrol.* **14**, 349-380.

Ebadi, A. & Johannes, W. (1991): Beginning of melting and composition of first melts in the system Qz–Ab–Or–H_2O–CO_2. *Contrib. Mineral. Petrol.* **106**, 286-295.

Emslie, R.F. (1978): Anorthosite massifs, rapakivi granites, and late Proterozoic rifting of North America. *Precambrian Res.* **7**, 61-98.

——— (1987): Mistastin batholith. *In* Radiogenic Age and Isotopic Studies, Report **1**. *Geol. Surv. Can.*, 146-148.

——— (1991): Granitoids of rapakivi-anorthosite and related associations. *Precambrian Res.* **51**, 173-192.

———, Cousens, B., Hamblin, C. & Bielecki, J. (1980): The Mistastin batholith, Labrador – Quebec: an Elsonian composite rapakivi suite. *Geol. Surv. Can., Pap.* **80-1A**, 95-100.

——— & Hegner, E. (1993): Reconnaissance isotopic geochemistry of anorthosite – mangerite – charnockite – granite (AMCG) complexes, Grenville Province, Canada. *Chem. Geol.* **106**, 279-298.

——— & Loveridge, W.D. (1991): Geochronology, geochemistry and petrogenesis of granites associated with rapakivi granite – anorthosite, central Labrador. *Symp. on Rapakivi Granites and Related Rocks, Abstr. Vol.* (I. Haapala & O.T. Rämö, eds.). *Geol. Surv. Finland, Guide* **34**, 15.

——— & ——— (1992): Fluorite-bearing early and middle Proterozoic granites, Okak Bay area, Labrador: geochronology, geochemistry and petrogenesis. *Lithos* **28**, 87-109.

——— & Russell, W.J. (1988): Umiakovik Lake batholith and other felsic intrusions, Okak Bay area, Labrador. *Geol. Surv. Can., Pap.* **88-1C**, 27-32.

——— & Thériault, R.J. (1991): Sm–Nd and Rb–Sr isotopic characteristics of ferrodiorites and related rocks associated with anorthositic complexes, central Labrador. *Geol. Assoc. Can. – Mineral. Assoc. Can., Program Abstr.* **16**, A34.

Evensen, N.M., Hamilton, P.J. & O'Nions, R.K. (1978): Rare-earth abundances in chondritic meteorites. *Geochim. Cosmochim. Acta* **42**, 1199-1212.

FROST, B.R. & LINDSLEY, D.H. (1992): Equilibria among Fe–Ti oxides, pyroxenes, olivine, and quartz. II. Application. *Am. Mineral.* **77**, 1004-1020.

———, ——— & ANDERSEN, D.J. (1988): Fe–Ti oxide – silicate equilibria: assemblages with fayalitic olivine. *Am. Mineral.* **73**, 727-740.

FUHRMAN, M.L. & LINDSLEY, D.H. (1988): Ternary-feldspar modeling and thermometry. *Am. Mineral.* **73**, 201-215.

GHENT, E.D., NICHOLLS, J., SIMONY, P.S., SEVIGNY, J.H. & STOUT, M.Z. (1991): Hornblende geobarometry of the Nelson Batholith, southeastern British Columbia: tectonic implications. *Can. J. Earth Sci.* **28**, 1982-1991.

HAMILTON, M.A. & SHIREY, S.B. (1992): Nd and Sr isotopic variations in anorthositic rocks of the Nain Plutonic Suite, Labrador. *Am. Geophys. Union, Trans.* **73**, 355 (abstr.).

HEWITT, D.A. & WONES, D.R. (1984): Experimental phase relations of the micas. *In* Micas (S.W. Bailey, ed.). *Rev. Mineral.* **13**, 201-256.

HILL, J.D. (1982): Geology of the Flowers River – Notakwanon River area, Labrador. *Mineral Development Div., Newfoundland Dep. Mines and Energy, Rep.* **82-6**.

HOLLISTER, L.S., GRISSOM, G.C., PETERS, E.K., STOWELL, H.H. & SISSON, V.B. (1987): Confirmation of the empirical correlation of Al in hornblende with pressure of solidification of calc-alkaline plutons. *Am. Mineral.* **72**, 231-239.

HUGHES, J.M., CAMERON, M. & CROWLEY, K.D. (1989): Structural variations in natural F, OH, and Cl apatites. *Am. Mineral.* **74**, 870-876.

JOHNSON, M.C. & RUTHERFORD, M.J. (1989): Experimental calibration of the aluminum-in-hornblende geobarometer with application to Long Valley caldera (California) volcanic rocks. *Geology* **17**, 837-841.

KOCH-MÜLLER, M., CEMIC, L. & LANGER, K. (1992): Experimental and thermodynamic study of Fe–Mg exchange between olivine and orthopyroxene in the system MgO–FeO–SiO_2. *Eur. J. Mineral.* **4**, 115-135.

LINDSLEY, D.H. (1983): Pyroxene thermometry. *Am. Mineral.* **68**, 477-493.

——— & FROST, B.R. (1992): Equilibria among Fe–Ti oxides, pyroxenes, olivine, and quartz. I. Theory. *Am. Mineral.* **77**, 987-1003.

———, ———, ANDERSEN, D.J. & DAVIDSON, P.M. (1990): Fe–Ti oxide – silicate equilibria: assemblages with orthopyroxene. *In* Fluid – Mineral Interactions: a Tribute to H.P. Eugster (R.J. Spencer & I-Ming Chou, eds.). *Geochem. Soc., Spec. Publ.* **2**, 103-119.

MORSE, S.A. (1992): Partitioning of strontium between plagioclase and melt: a comment. *Geochim. Cosmochim. Acta* **56**, 1735-1737.

——— & HAMILTON, M.A. (1991): The problem of unsupported radiogenic strontium in the Nain anorthosites, Labrador. *In* Mid-Proterozoic Laurentia–Baltica (C.F. Gower, T. Rivers & B. Ryan, eds.). *Geol. Assoc. Can., Spec. Pap.* **38**, 373-385.

MUNOZ, J.L. & SWENSON, A. (1981): Chloride – hydroxyl exchange in biotite and estimation of relative HCl/HF activities in hydrothermal fluids. *Econ. Geol.* **76**, 2212-2221.

MYERS, J. & EUGSTER, H.P. (1983): The system Fe–Si–O: oxygen buffer calibrations to 1,500 K. *Contrib. Mineral. Petrol.* **82**, 75-90.

NANEY, M.T. (1983): Phase equilibria of rock-forming ferromagnesian silicates in granitic systems. *Am. J. Sci.* **283**, 993-1033.

NEKVASIL, H. (1990): Reaction relations in the granite system: implications for trachytic and syenitic magmas. *Am. Mineral.* **75**, 560-571.

——— (1991): Ascent of felsic magmas and formation of rapakivi. *Am. Mineral.* **76**, 1279-1290.

OLSON, K.E. & MORSE, S.A. (1990): Regional Al–Fe mafic magmas associated with anorthosite-bearing terranes. *Nature* **344**, 760-762.

PASTEELS, P., DEMAIFFE, D. & MICHOT, J. (1979): U–Pb and Rb–Sr geochronology of the eastern part of the south Rogaland igneous complex, southern Norway. *Lithos* **12**, 199-208.

POUCHOU, J.L. & PICHOIR, F. (1984): A new model for quantitative X-ray microanalysis. *La Recherche Aerospatiale* **3**, 167-192.

PUZIEWICZ, J. & JOHANNES, W. (1990): Experimental study of a biotite-bearing granitic system under water-saturated and water-undersaturated conditions. *Contrib. Mineral. Petrol.* **104**, 397-406.

RÄMÖ, O.T. (1991): Petrogenesis of the Proterozoic rapakivi granites and related basic rocks of southeastern Fennoscandia: Nd and Pb isotopic and general geochemical constraints. *Geol. Surv. Finland, Bull.* **355**.

RØNSBO, J.G. (1989): Coupled substitutions involving REEs and Na and Si in apatites in alkaline rocks from the Ilímaussaq intrusion, south Greenland, and the petrological implications. *Am. Mineral.* **74**, 896-901.

RUDNICK, R.L. (1992): Restites, Eu anomalies, and the lower continental crust. *Geochim. Cosmochim. Acta* **56**, 963-970.

RYAN, B. (1991): Makhavinekh Lake Pluton, Labrador, Canada: geological setting, subdivisions, mode of emplacement, and a comparison with Finnish rapakivi granites. *Precambrian Res.* **51**, 193-225.

———, KROGH, T.E., HEAMAN, L., SCHÄRER, U., PHILIPPE, S. & OLIVER, G. (1991): On recent geochronological

studies in the Nain Province, Churchill Province and Nain Plutonic Suite, north-central Labrador. *Newfoundland Dep. Mines and Energy, Geol. Surv. Branch, Rep.* **91-1**, 257-261.

SIMMONS, K.R. & SIMMONS, E.C. (1987): Petrogenetic implications of Pb- and Sr-isotopic compositions for rocks from the Nain anorthosite complex, Labrador. *Geol. Soc. Am., Abstr. Programs* **19**, 845.

———, WIEBE, R.A., SNYDER, G.A. & SIMMONS, E.C. (1986): U–Pb zircon age for the Newark Island layered intrusion, Nain anorthosite complex, Labrador. *Geol. Soc. Am., Abstr. Programs* **18**, 751.

SMITH, D. (1971): Stability of the assemblage iron-rich orthopyroxene – olivine – quartz. *Am. J. Sci.* **271**, 370-382.

——— (1974): Pyroxene – olivine – quartz assemblages in rocks associated with the Nain anorthosite massif, Labrador. *J. Petrol.* **15**, 58-78.

STIMAC, J.A. & WARK, D.A. (1992): Plagioclase mantles on sanidine in silicic lavas, Clear Lake, California: implications for the origin of rapakivi texture. *Geol. Soc. Am. Bull.* **104**, 728-744.

SUOMINEN, V. (1991): The chronostratigraphy of southwestern Finland with special reference to Postjotnian and Subjotnian diabases. *Geol. Surv. Finland, Bull.* **356**.

TAYLOR, F.C. (1978): Umiakovik Lake adamellite pluton, northern Labrador. *In* Rubidium–Strontium Isochron Age Studies, Report 2 (R.K. Wanless & W.D. Loveridge, eds.). *Geol. Surv. Can., Pap.* **77-14**, 50-51.

——— (1979): Reconnaissance geology of a part of the Precambrian Shield, northeastern Quebec, northern Labrador, and Northwest Territories. *Geol. Surv. Can., Mem.* **393**.

TAYLOR, S.R., CAMPBELL, I.H., MCCULLOCH, M.T. & MCLENNAN, S.M. (1984): A lower crustal origin for massif-type anorthosites. *Nature* **311**, 372-374.

TSVETKOV, A.A. & SUKHANOV, M.K. (1991): High-alumina mafic magmas – models and reality. *Int. Geol. Rev.* **33**, 174-190.

VAASJOKI, M., RÄMÖ, O.T. & SAKKO, M. (1991): New U–Pb ages from the Wiborg rapakivi area: constraints on the temporal evolution of the rapakivi granite – anorthosite – diabase dyke association of southeastern Finland. *Precambrian Res.* **51**, 227-243.

VOLFINGER, M., ROBERT, J.-L., VIELZEUF, D. & NEIVA, A.M.R. (1985): Structural control of the chlorine content of OH-bearing silicates (micas and amphiboles). *Geochim. Cosmochim. Acta* **49**, 37-48.

WEDEPOHL, K.H. (1991): Chemical composition and fractionation of the continental crust. *Geol. Rund.* **80**, 207-223.

WHEELER, E.P., 2ND (1933): A study of some diabase dykes on the Labrador coast. *J. Geol.* **41**, 418-431.

——— (1942): Anorthosite and associated rocks about Nain, Labrador. *J. Geol.* **50**, 611-642.

——— (1955): Adamellite intrusive north of Davis Inlet, Labrador. *Geol. Soc. Am. Bull.* **66**, 1031-1060.

——— (1960): Anorthosite – adamellite complex of Nain, Labrador. *Geol. Soc. Am. Bull.* **71**, 1755-1762.

——— (1969): Minor intrusives associated with the Nain anorthosite. *In* Origin of Anorthosite and Related Rocks (Y.W. Isachsen, ed.). *N.Y. State Mus. and Sci. Service, Mem.* **18**, 189-206.

WIEBE, R.A. (1978): Anorthosite and associated plutons, southern Nain complex, Labrador. *Can. J. Earth Sci.* **15**, 1326-1340.

——— (1980): Commingling of contrasted magmas in the plutonic environment: examples from the Nain anorthositic complex. *J. Geol.* **88**, 197-209.

——— & WILD, T. (1983): Fractional crystallization and magma mixing in the Tigalak layered intrusion, the Nain anorthosite complex, Labrador. *Contrib. Mineral. Petrol.* **84**, 327-344.

WONES, D.R. (1981): Mafic silicates as indicators of intensive variables in granitic magmas. *Mining Geol.* **31**, 191-212.

——— (1989): Significance of the assemblage titanite + magnetite + quartz in granitic rocks. *Am. Mineral.* **74**, 744-749.

——— & EUGSTER, H.P. (1965): Stability of biotite: experiment, theory, and application. *Am. Mineral.* **50**, 1228-1272.

WOOD, B.J., NELL, J. & WOODLAND, A.B. (1991): Macroscopic and microscopic thermodynamic properties of oxides. *In* Oxide Minerals: Petrologic and Magnetic Significance (D.H. Lindsley, ed.). *Rev. Mineral.* **25**, 265-302.

Received July 2, 1992, revised manuscript accepted June 2, 1993.

APPENDIX 2.
SAMPLE LOCATIONS, UTM COORDINATES (ALL IN ZONE 20)

UMIAKOVIK	East	North
monzodiorites		
EC87-54	521350	6354850
EC87-86	522620	6353040
EC90-250A	513950	6297230
fa-px-qtz monzonites		
EC89-302	516200	6346100
EC89-308	504800	6342900
EC89-311	492600	6379800
EC89-324	497400	6349000
EC89-363	507000	6311200
EC90-228	519390	6300870
EC90-253	503760	6291730
hbl and bt-hbl granites		
EC87-100 bt-hbl	507160	6364920
EC87-106 bt-hbl	507600	6365660
EC87-119 bt-hbl	509440	6362430
EC87-152A topaz-bearing dyke	497000	6360600
EC89-323 bt-hbl	498600	6356600
EC89-342 hbl	474200	6335100
EC89-345 hbl	477700	6342700
MAKHAVINEKH		
olivine-bearing facies		
EC90-262	547970	6253460
EC90-263	549960	6252310
EC90-264	535360	6252240
olivine-free facies		
EC89-225	518300	6259000
EC89-226	514600	6257600
EC89-229	519700	6262200
NOTAKWANON		
fayalite-pyroxene granites		
EC89-110	570510	6171600
EC89-117	570620	6198200
EC89-119	570220	6190700
EC89-125	570050	6175400
EC89-128	558600	6175700
VOISEY BAY		
fayalite-bearing granite		
EC90-191	564050	6230670
bi-hb granite		
EC90-187	602000	6221740
EC90-190	560710	6231230
EC90-193	576980	6231520
OTHER NPS GRANITOIDS		
EC90-105	614720	6280080
EC90-106	613910	6279680
EC90-108	614950	6282470
EC90-179	611640	6272600
EC90-181	624250	6220570
EC90-234	527490	6273090
EC90-236	526920	6274200
EC90-143	558240	6277750
EC90-161	556980	6277390

APPENDIX 3.
CALCULATION OF MINERAL EQUILIBRIA

Fe^{3+} in biotite

Any attempts to calculate Fe^{3+} in biotite based on charge balance requires assumptions not easy to justify; thus a less subjective procedure was developed. An estimate of Fe^{3+} was made using the following rationale. Compositions of igneous biotite from the literature were sought in which Fe^{3+} and Fe^{2+} had been determined and in which Fe^{3+} and Fe^{2+} of the host rock also had been measured. Biotite – whole rock pairs in which the biotite was found to have Fe/(Fe+Mg) greater than 0.50 were especially pursued. A total of 366 pairs was collected from the literature and subjected to stepwise multiple linear regression. A wide range of cation components and site occupancies were input as independent variables. A final equation was fitted as follows:

$$(Fe^{3+}/Fe_{tot}) \text{ in biotite} = 0.404(Fe_{tot}) \text{ in the rock} + 0.012\ Fe_{tot} \text{ in biotite} - 0.061\ {}^{VI}Ti \text{ in biotite}$$

Activity models

Activity models used for solid solutions involved in the reactions considered were as follows:

aOr in alkali feldspar: calculated from the model of Fuhrman & Lindsley (1988).

aMt in spinel: calculated using the model of Wood *et al.* (1991).

aAnn in biotite: taken as equal to $(X Fe^{2+})^3 \cdot (XOH)^2$, as proposed by Czamanske & Wones (1973). Fe^{3+} estimated from relationship described above.

aFa in olivine: taken as equal to $XFe/(XFe+XMg)$ in olivine.